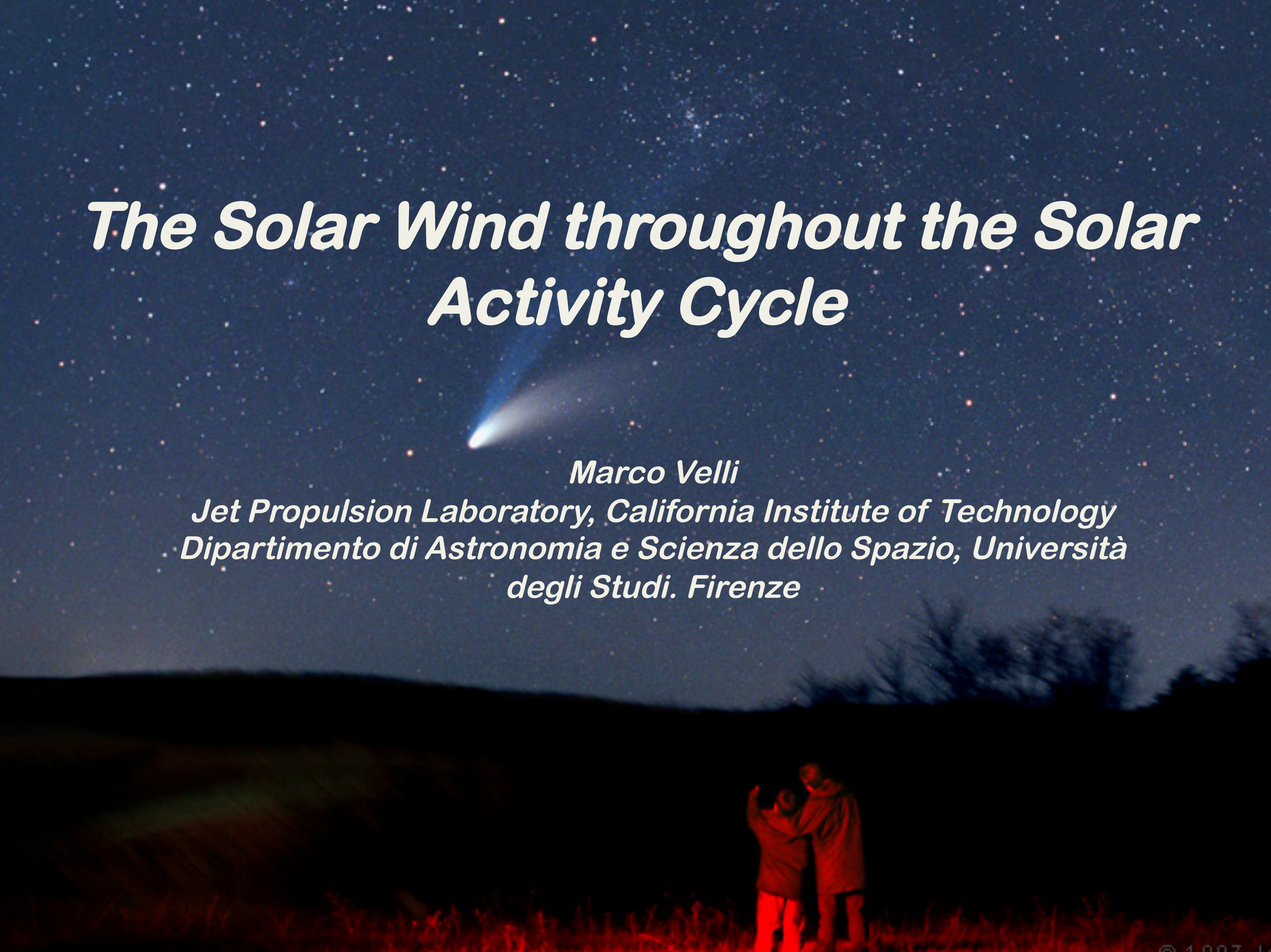

The Solar Wind throughout the Solar Activity Cycle

Marco Velli
Jet Propulsion Laboratory, California Institute of Technology
Dipartimento di Astronomia e Scienza dello Spazio, Università degli Studi. Firenze

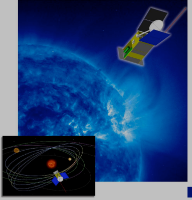

Outline

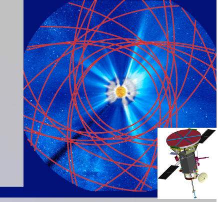

- The solar wind throughout the activity cycle: geography
- Coronal heating and solar wind acceleration
- Source region and dynamics of the fast wind
- What is the role of turbulence and Alfvénic turbulence in particular?
- Fast solar wind: fine structures: microstreams; polar plumes?
- Slow solar wind origins
- Solar Probe/Solar Orbiter

The Solar Wind at ULYSSES

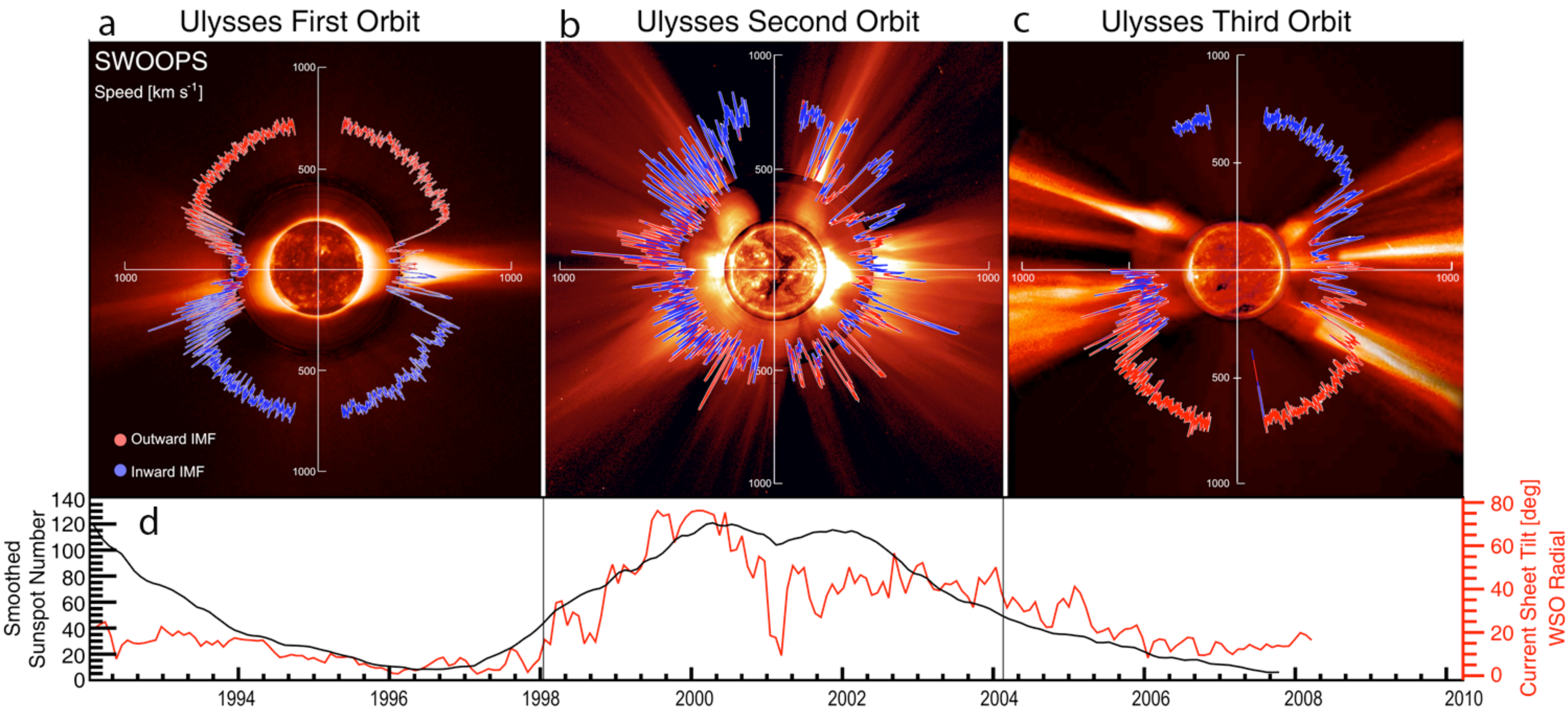

Evolution to the new solar minimum: correlation of wind and magnetic field structure

ULYSSES over 3 cycles

v_p (km/s)	761	739	3%
v_α (km/s)	772	746	3%
n_pR^2 (cm^3)	2.65	2.19	17%
$n_\alpha R^2$ (cm3)	0.12	0.10	17%
T_pR 105 (K)	2.66	2.30	14%
T_aR 106 (K)	1.12	1.00	11%
Mass Flux (kg/m^2s)			
$\rho VR^2 * 10^{15}$	3.96	3.17	20%
Dynamic Pressure			
(nPa) ρV^2R^2	3.01	2.34	22%
Proton Thermal Pressure (pPa)			
$n_pkT_pR^3$	9.89	7.43	25%
Alpha Particle Thermal Pressure (pPa)			
$n_akT_aR^3$	1.80	1.39	23%

McComas et al. 08)

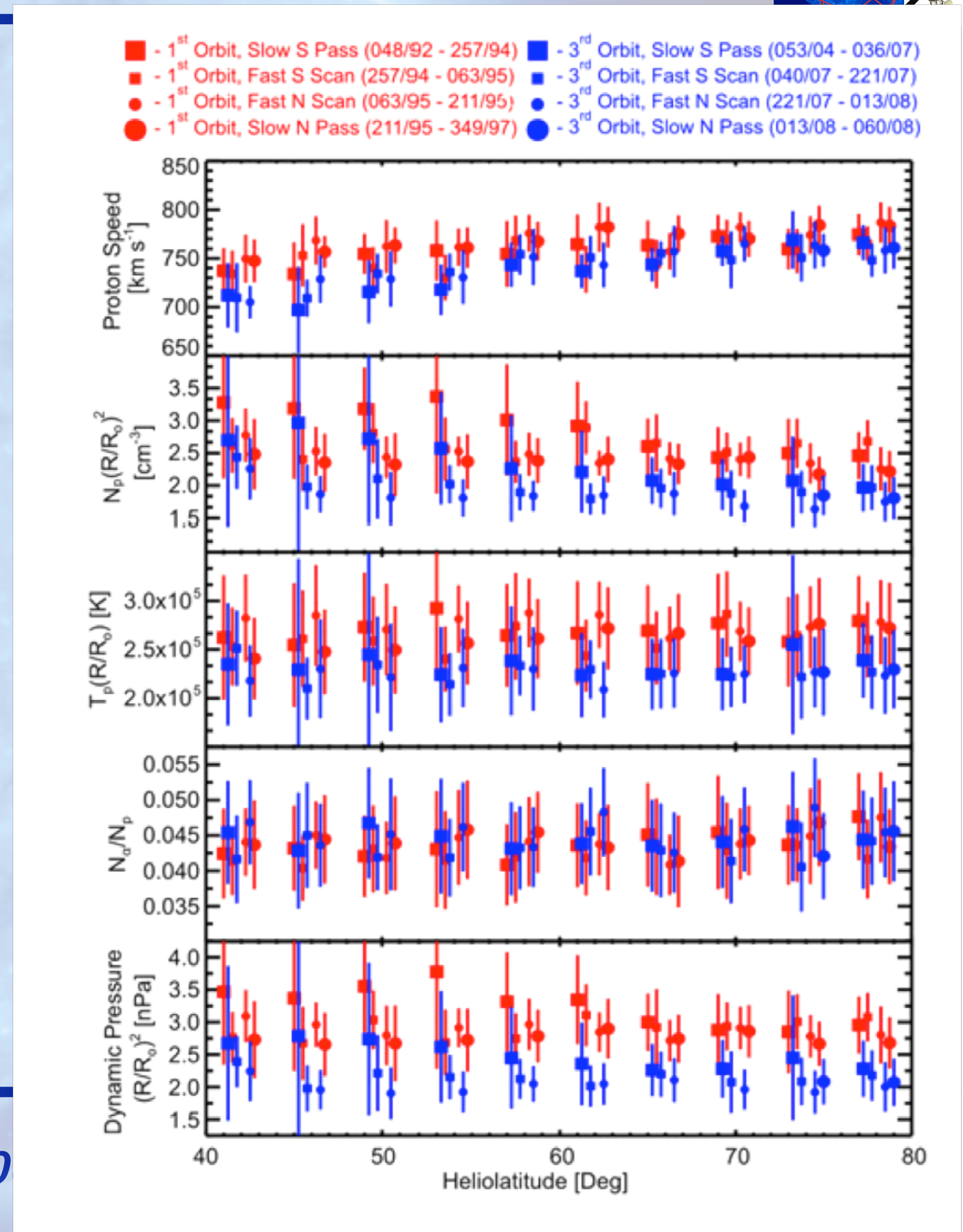

Coronal fine structure and its evolution into the solar wind

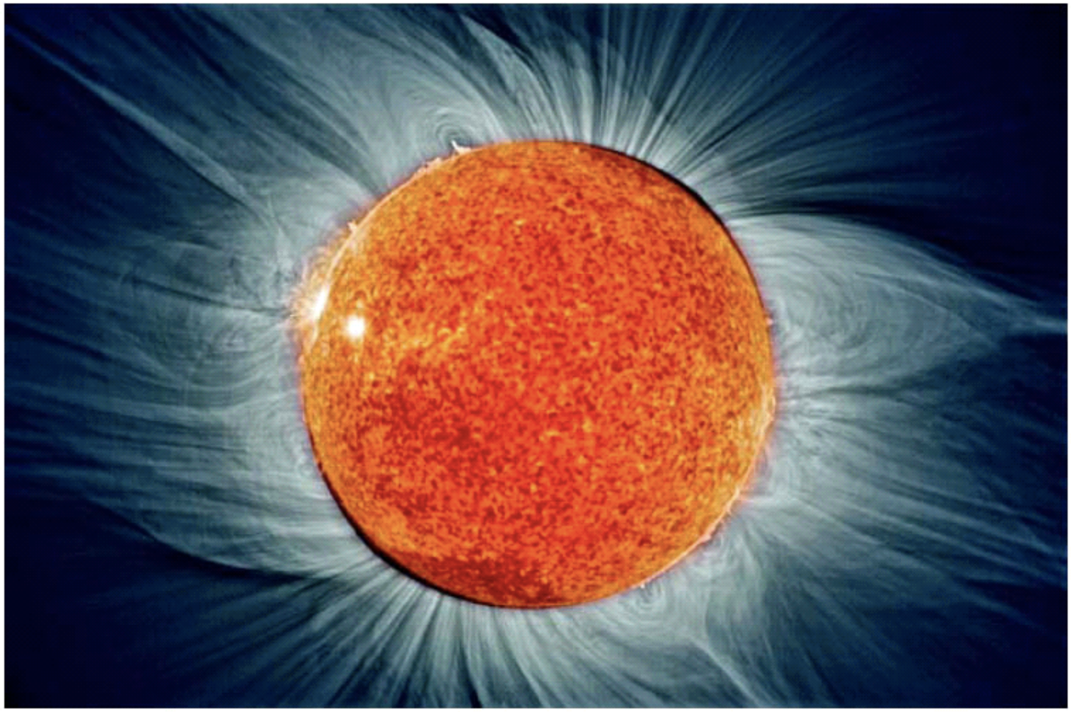

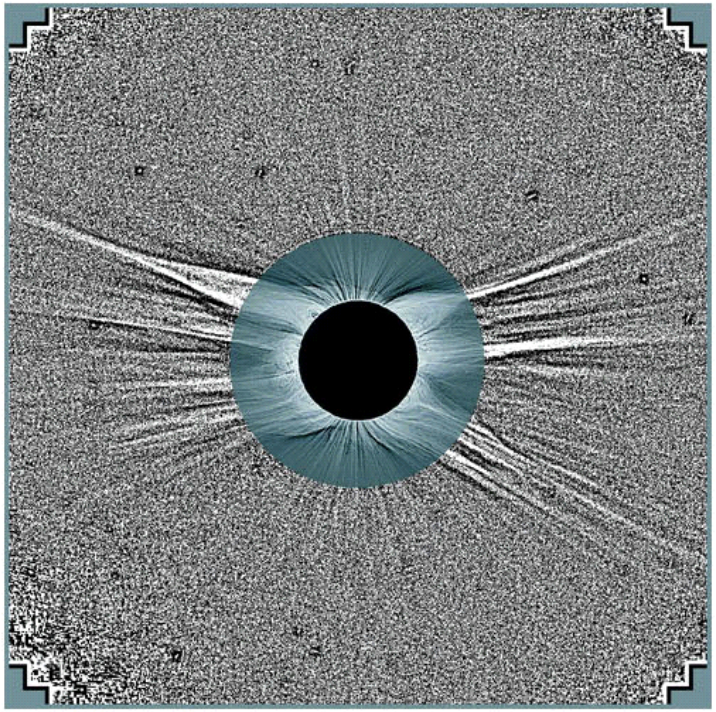

(a) White light eclipse 2007 March 29 corona made by a 1600 mm telescope in Libya and *SOHO EIT He II (30.4 nm). The resolution of the image is 1-2" and its effective* wavelength within 400 - 650 nm. (b) Edge-enhanced Druckmüller-Aniol eclipse picture Lybia, 2006, cropped at r 1/4 2:2 Rs joined to a LASCO C2 image recorded at 10:46 UT. An unsharp mask has been applied to the LASCO white-light image by subtracting from it a smoothed version of itself. Image rotated about 30o cc compared to (a), From Pasachoff et al. (2007) andWang et al. (2007).

Solar Wind Distribution in Ecliptic

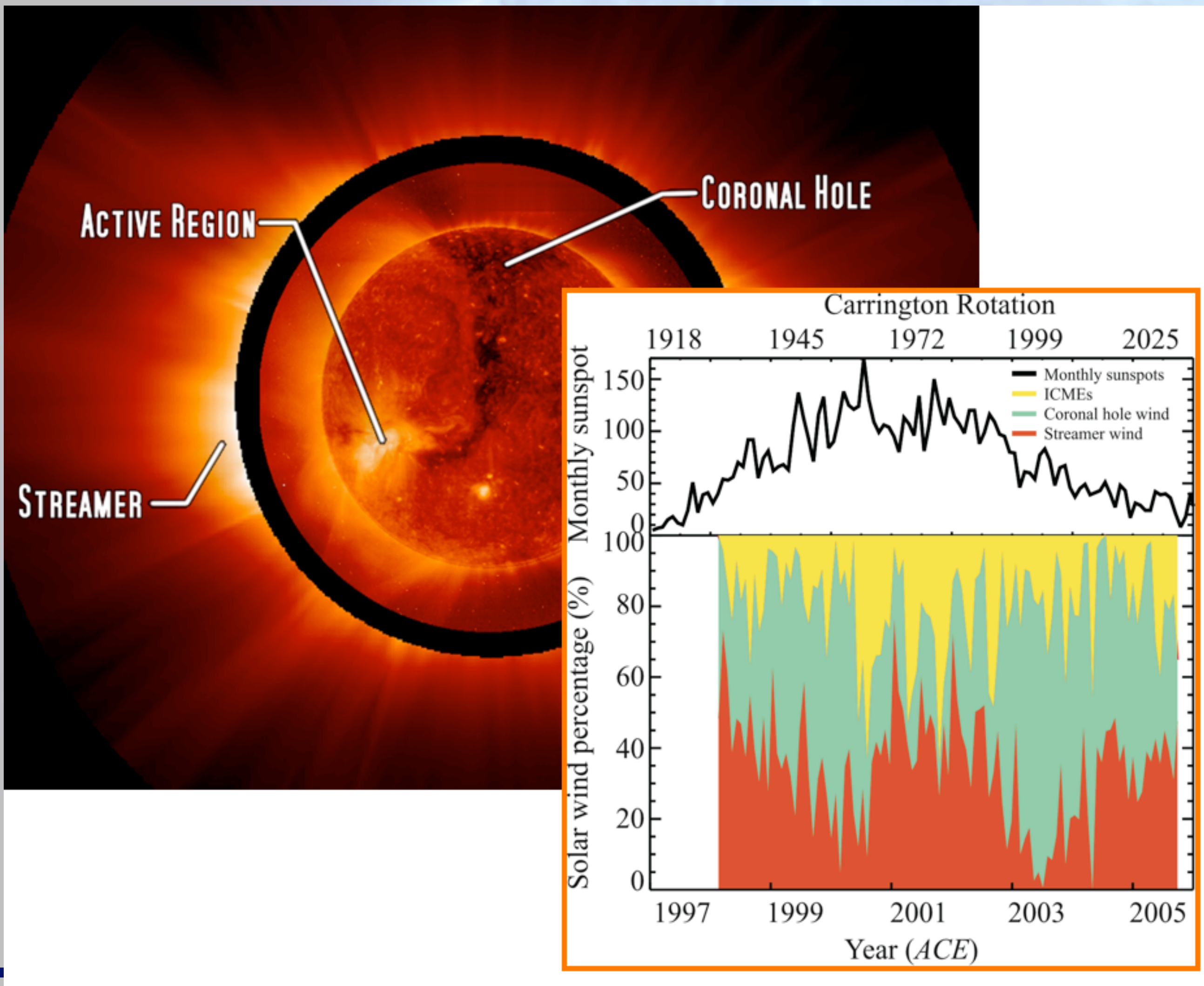

ACE data show that:

10s % each:

- ICME
- Coronal Hole
- Streamer Belt

(Zurbuchen et al. 06)

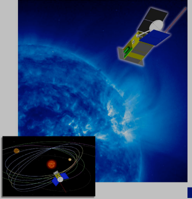

Solar Wind Acceleration Properties

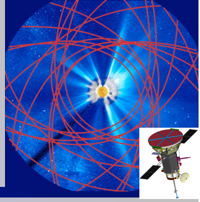

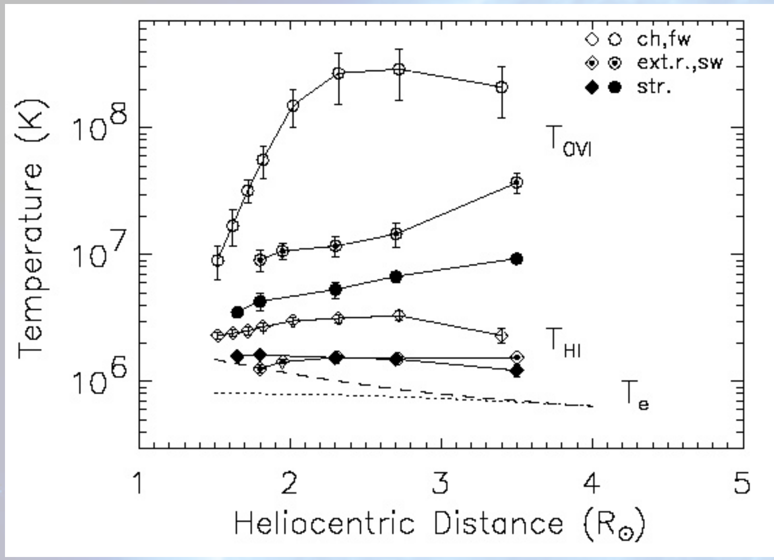

Antonucci , SSR 2006

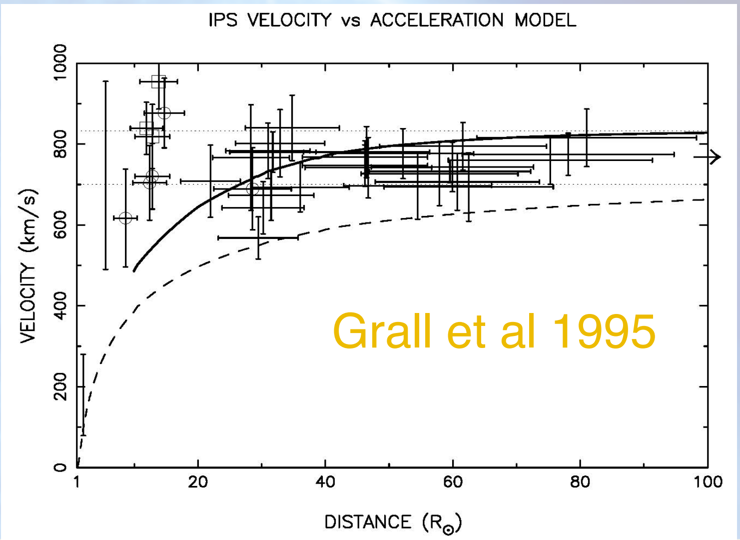

	fast	slow
speed (km/s)	600–800	300–500
T_p (10^5 K)	2.4	0.4
T_e (10^5 K)	1.0	1.3
T_{ion} / T_p	> m_{ion}/m_p	< m_{ion}/m_p
O^{7+}/O^{6+},Mg/O	low	high

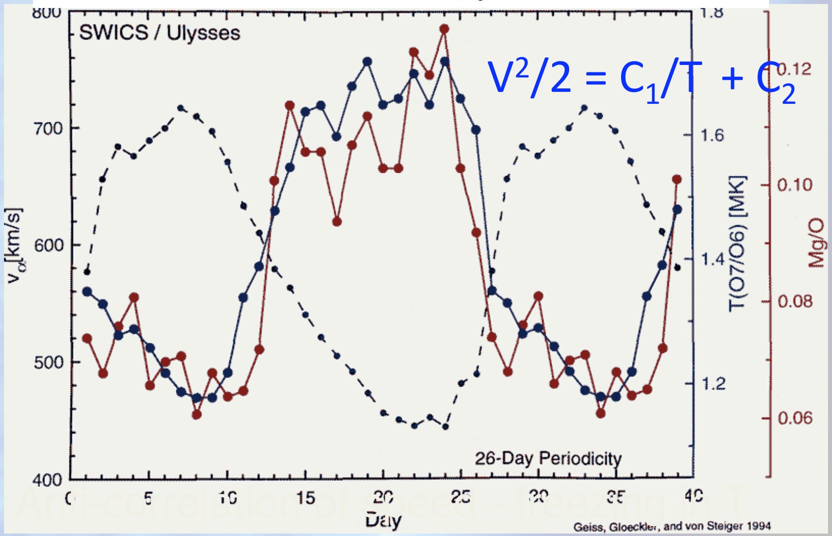

Solar Wind Speed and Helium Abundance

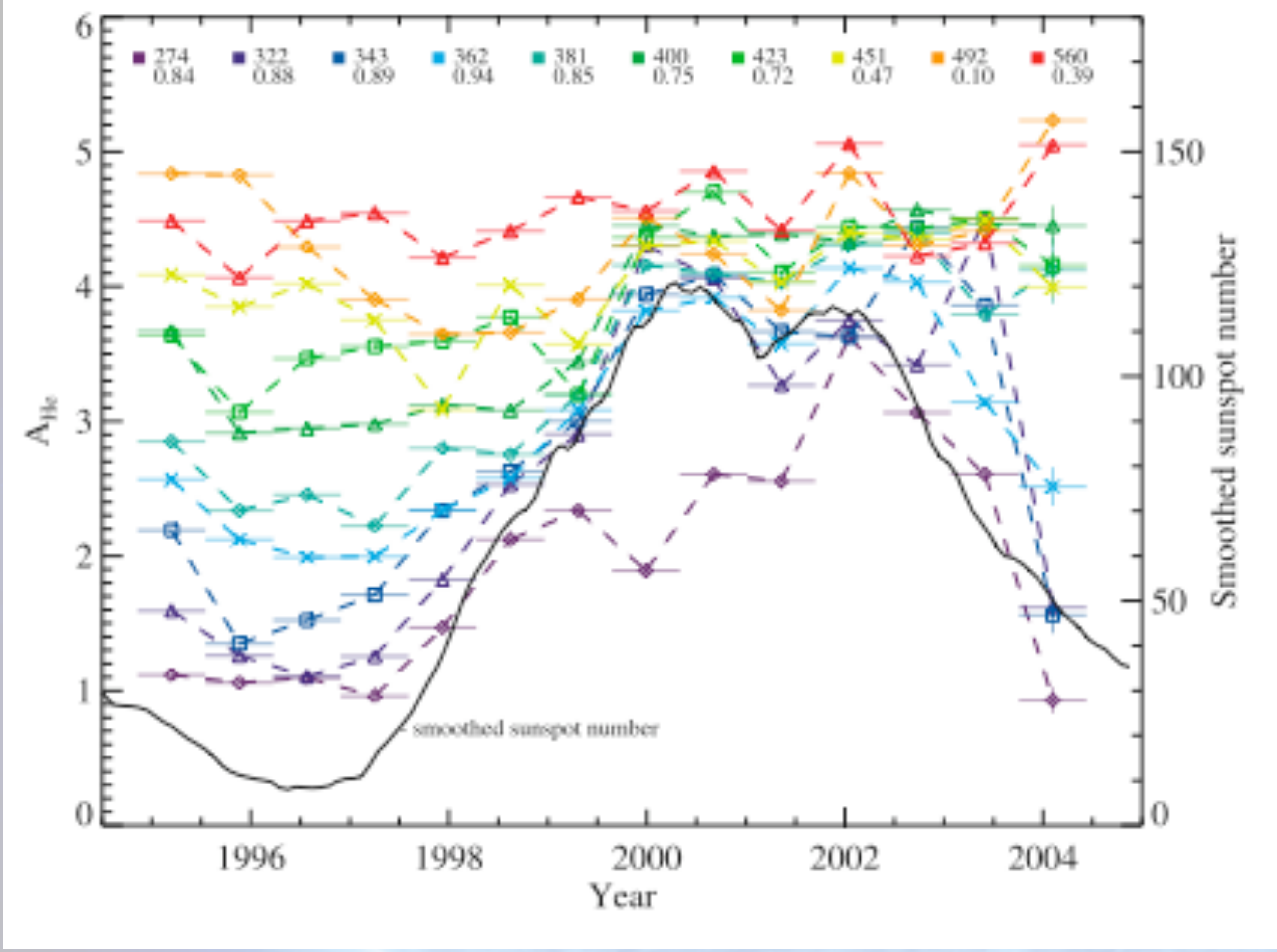

Average values of AHe over 250 day intervals and the smoothed sunspot number over the duration of the Wind mission. The legend lists the lower end of each speed window and the correlation coefficient between the averages and the smoothed sunspot number. The relative abundance of helium in the slow solar wind is strongly correlated with solar activity with a peak correlation of 0.94 for speeds between 360 and 380 km/ s.

Kasper et al. '07 Heliospheric Helium Abundance

Solar wind proton distribution functions

Helios observations in the solar wind

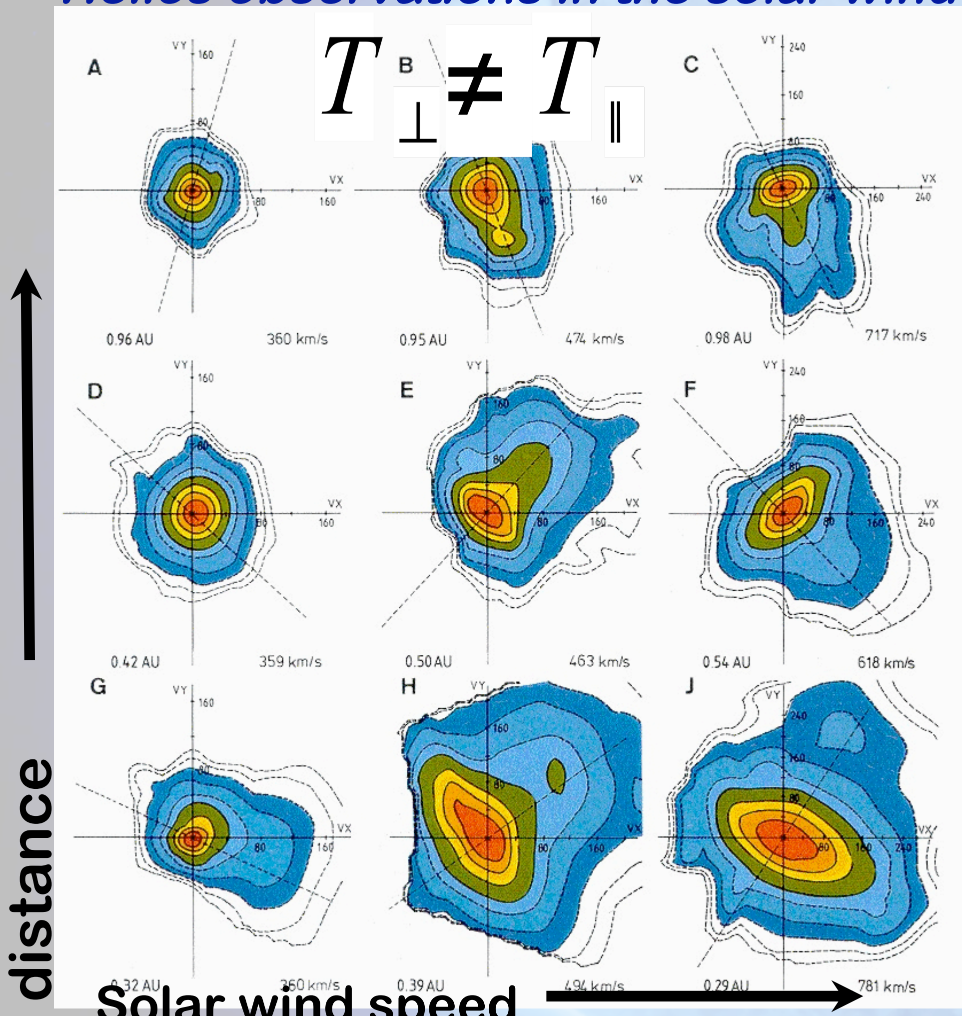

(*Marsch et al. 1982*)

Temperature anisotropy between parallel and perpendicular directions with respect to the ambient magnetic field

Velocity beam in the parallel direction

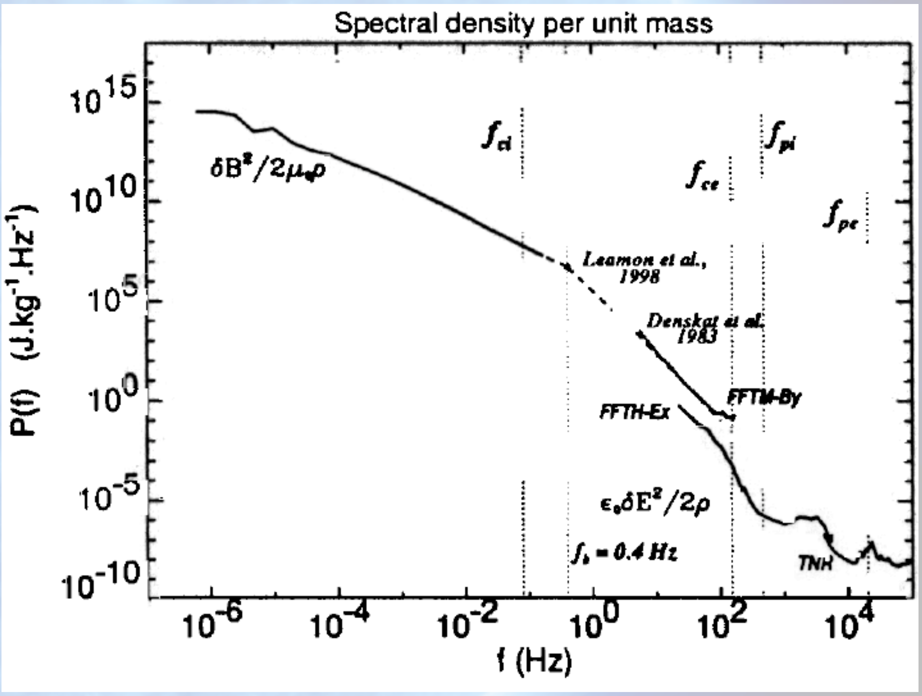

Spectrum of SW turbulence: Alfvén Waves and Alfvénic Turbulence

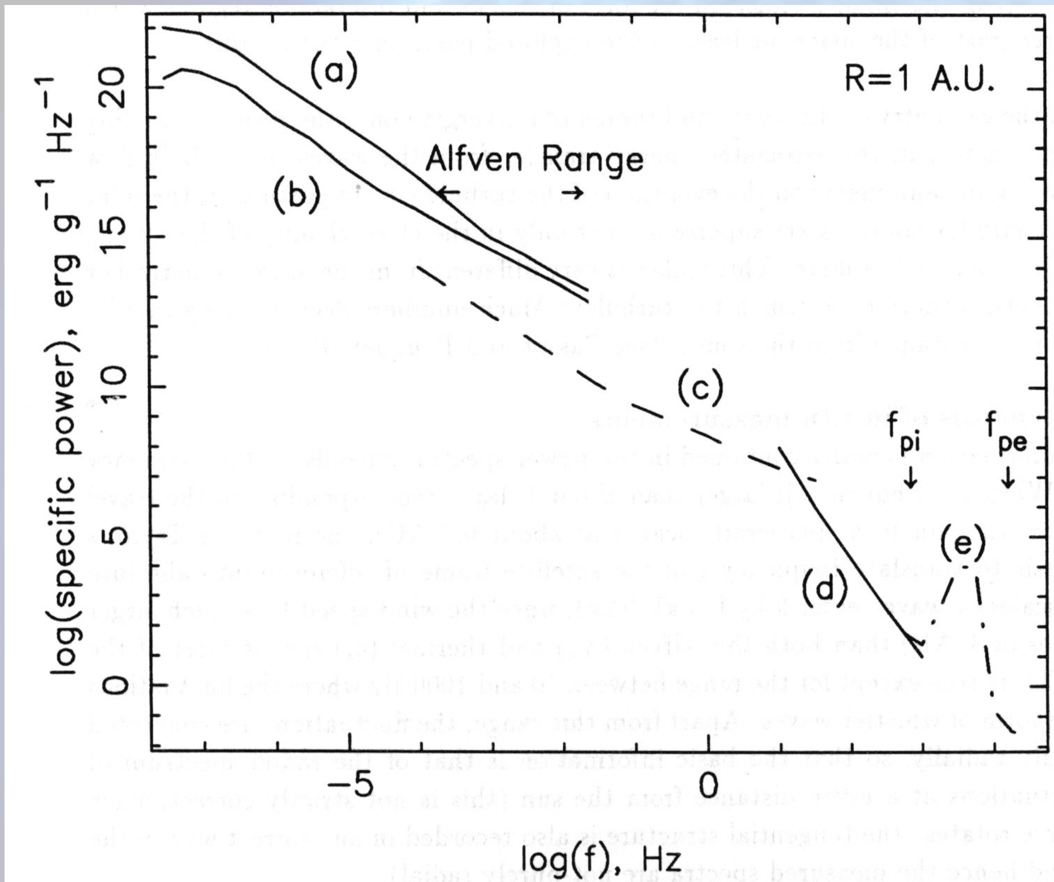

First recognized in solar wind fast streams by Belcher and Davis (1971) (10 -4 Hz < w < 10 -2 Hz) Transverse waves that propagate at the Alfvén speed

$$z^{\pm} = u \mp sign(B_r)b/\sqrt{4\pi\rho}$$

Turbulence in the inner heliosphere

Spectra of outward and inward waves, from Helios

Grappin et al. 1990

Between 0.3 and 1AU

Middle panel, wind speed.

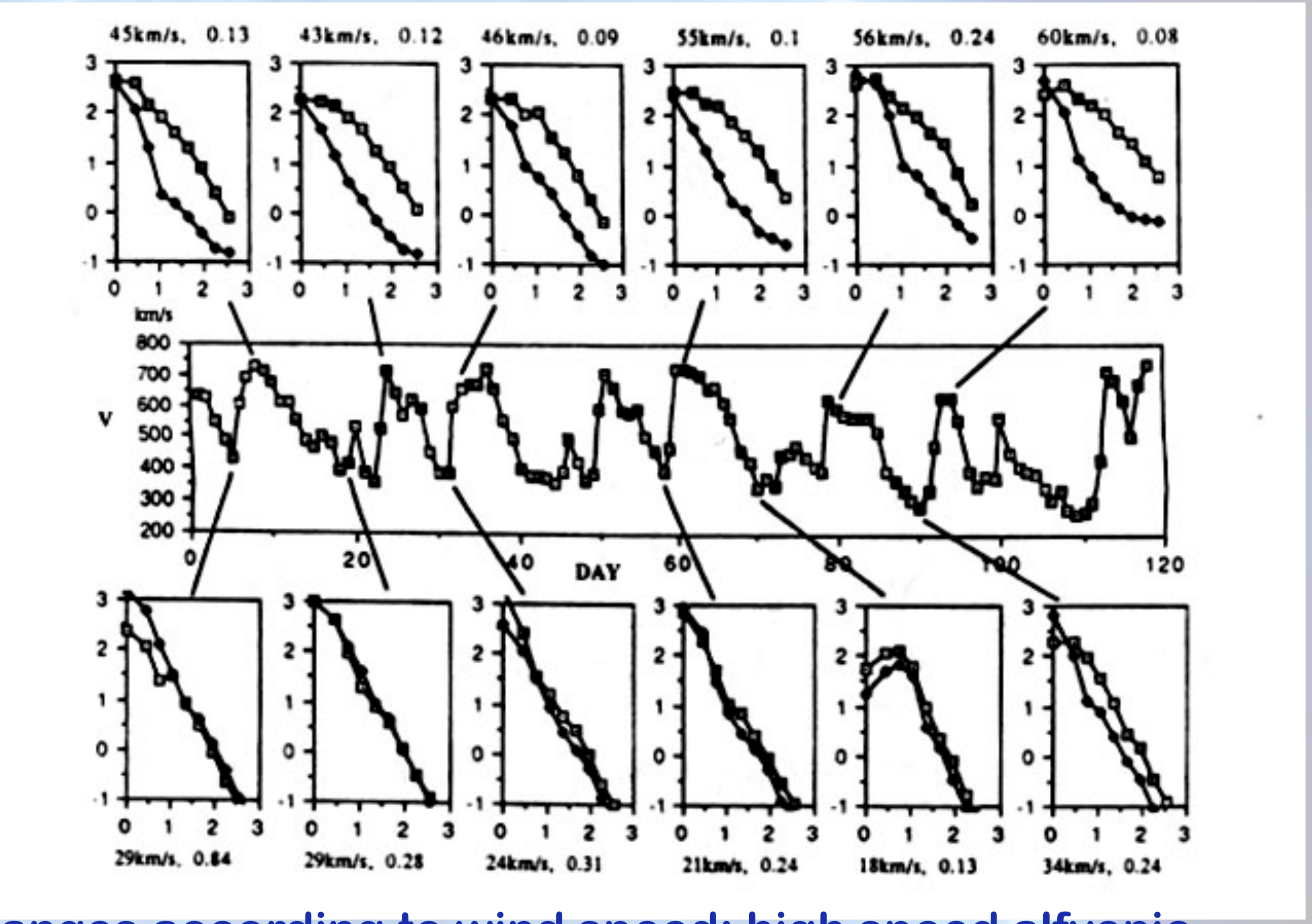

Turbulence changes according to wind speed: high speed alfvenic, low speed standard……where does this difference arise? What is the dynamical significance?

Turbulence (Helios results)

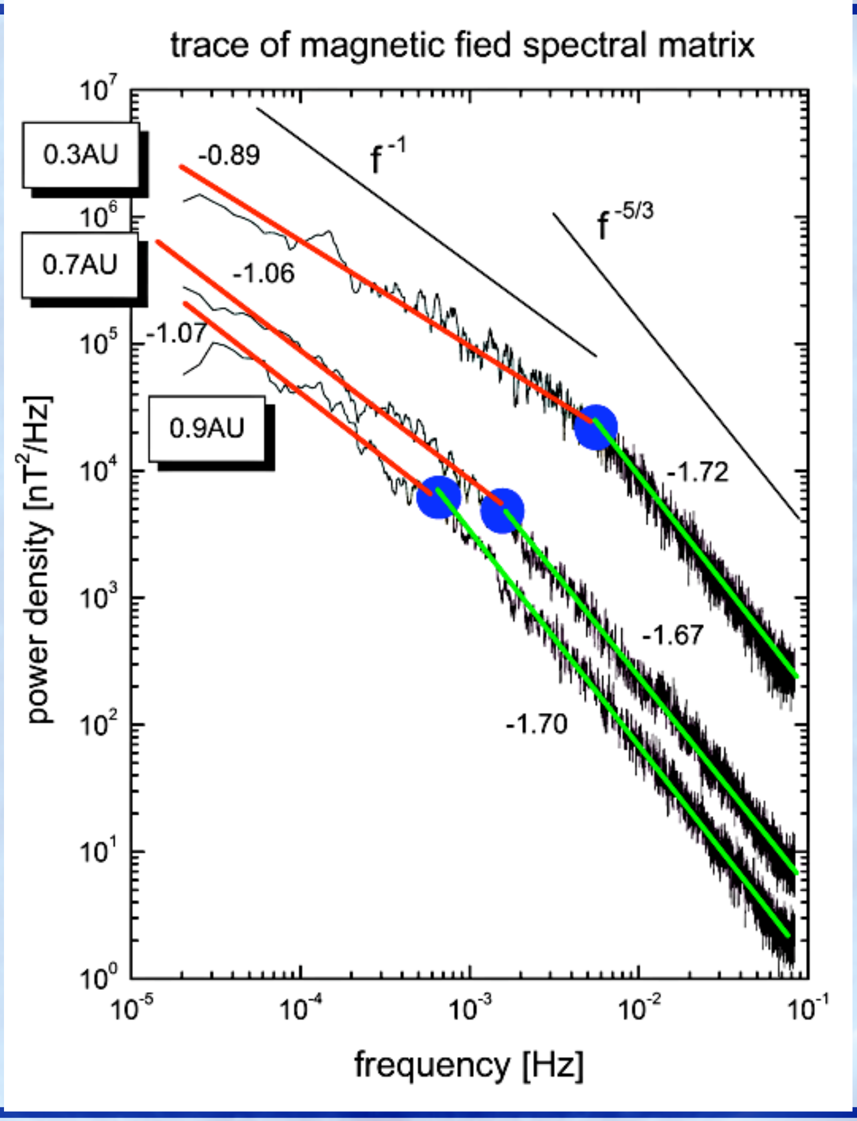

Evidence for the anisotropy of the Solar Wind Turbulence Cascade

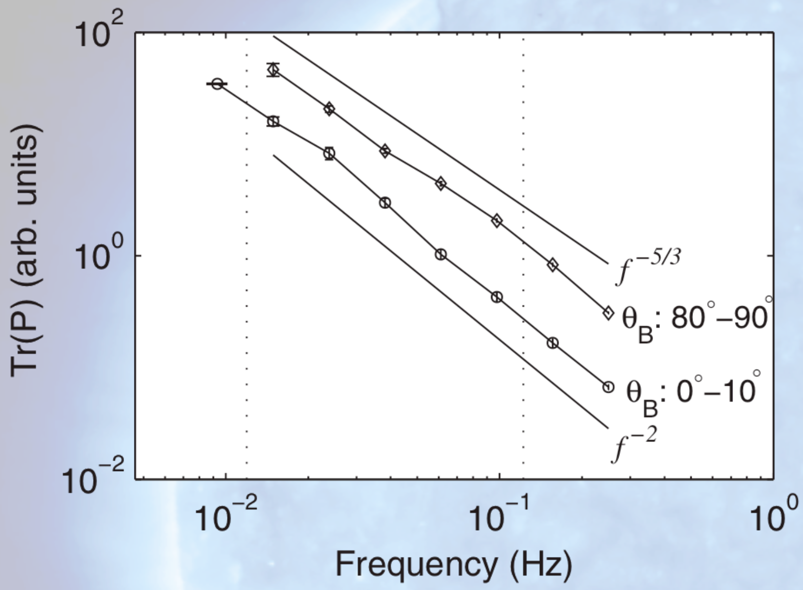

FIG. 1. Magnetic power spectra at two different angle ranges of the local magnetic field to the flow: 0°–10° (circles) and 80°–90° (diamonds). Note the reduced power levels and steeper slope associated with the smaller angle. Guide lines with slopes of 5/3 and 2 are shown above and below the data. Spectral indices in Fig. 2 are calculated over the scales between the dotted vertical lines.

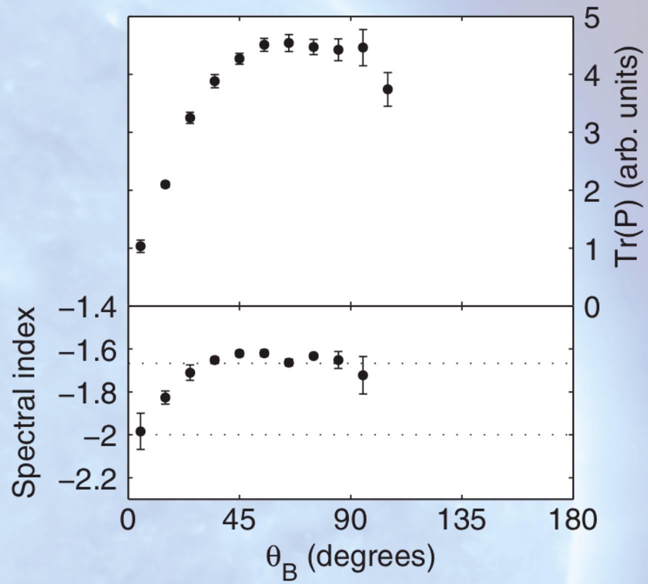

FIG. 2. Top: Trace of power in the magnetic field as a function of the angle between the local magnetic field and the sampling direction at a spacecraft frequency of 61 mHz. The larger scatter for $\theta_B > 90°$ is the result of fewer data points at these angles. Bottom: Spectral index of the trace, fitted over spacecraft frequencies from 15–98 mHz.

Horbury et al. 08, (also Podesta '09)

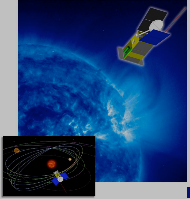

Turbulent heating of the solar wind

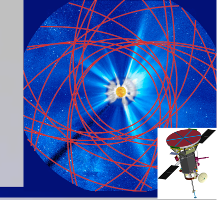

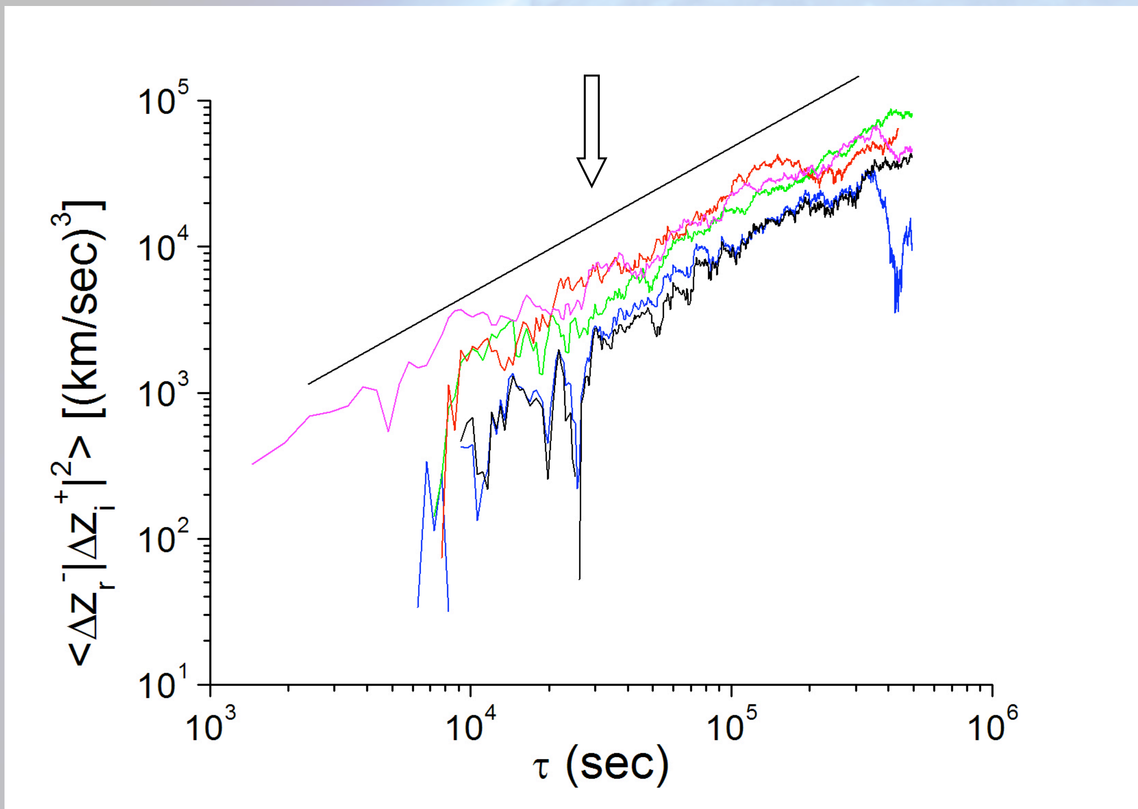

Observed scaling collapse onto the Yaglom law appears very robust in many periods of about 10 days.

(Low frequency) solar wind can be described in the framework of MHD turbulence

Taylor's hypothesis to transform length scales in time scales

$$\left\langle \Delta Z_r^{\mp} \left| \Delta Z_i^{\pm} \right|^2 \right\rangle = \frac{4}{3} V_{rms} \varepsilon^{\pm} \tau$$

L. Sorriso-Valvo et al., (2007)

Plasma instabilities driven by proton temperature anisotropy

$$\beta_{\|,\perp} = \frac{P_{\|,\perp}}{B_0/8\pi} = \frac{8\pi n k_B T_{\|,\perp}}{B_0^2}$$

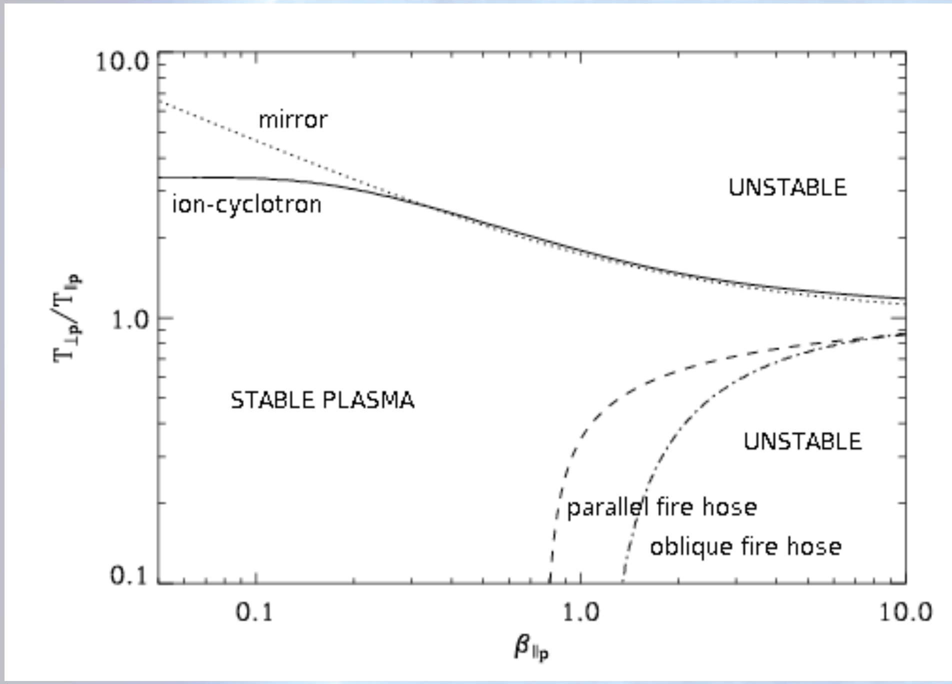

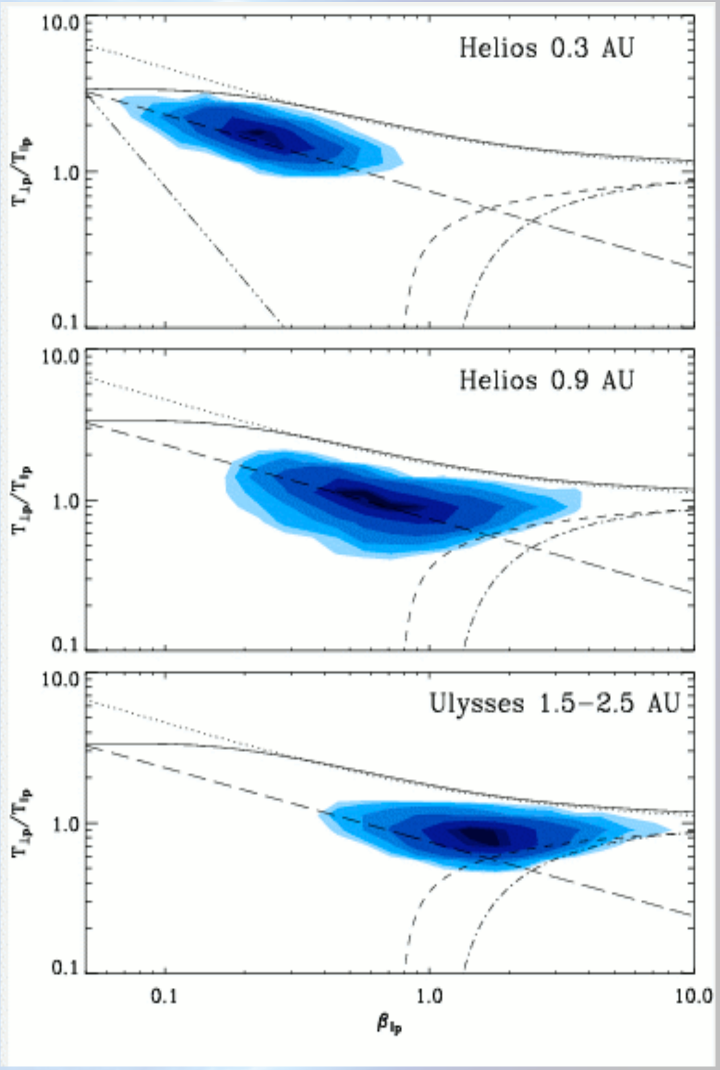

Energy flux balance

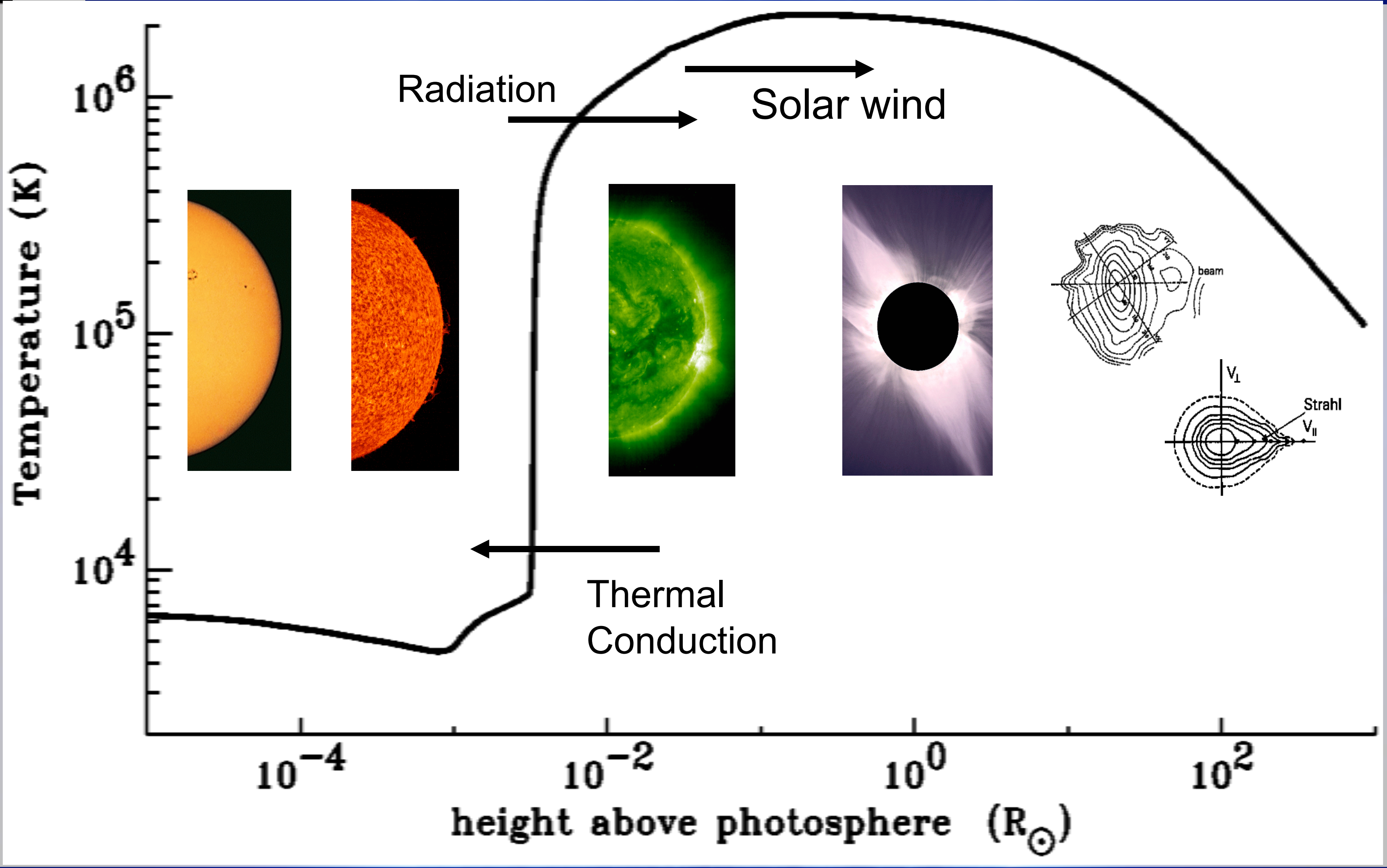

Basic Energy Balance Along a Flux Tube

Source Mechanical flux (Coronal Heating+Pressure) Conductive flux Radiative flux Solar Wind Flux:

$$F_0 = F_m + F_q + F_{rad} + F_{sw}$$

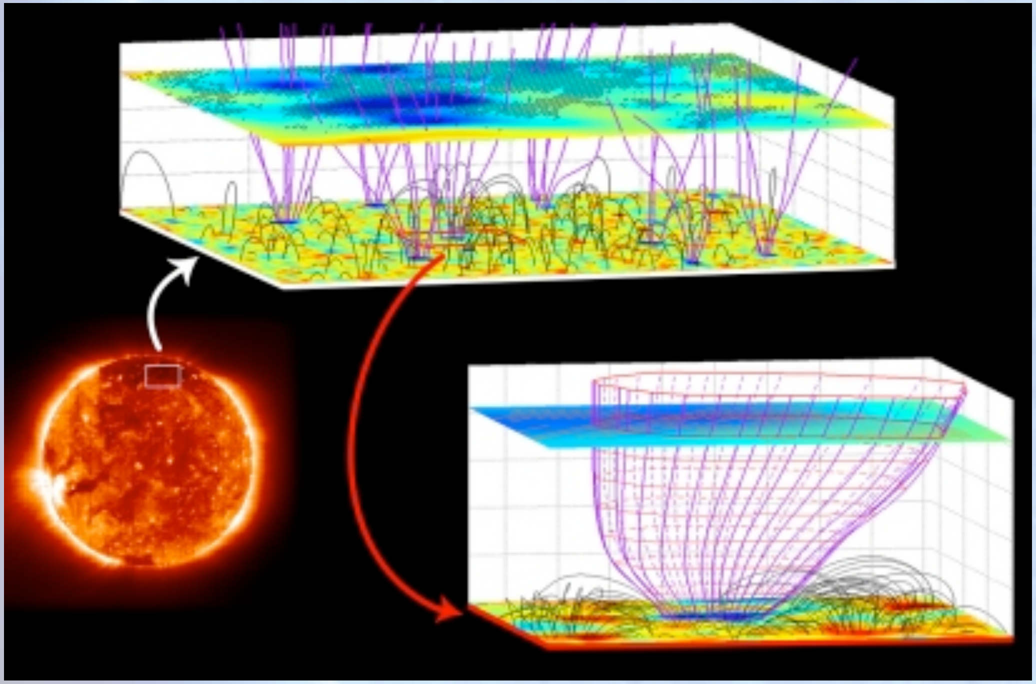

Source regions solar wind Marsch, Tu et al Science 2005

What is the source of mechanical flux?

Photospheric motions produce field line tangling and emerging flux resulting in a Poynting flux crossing the photosphere:

$$\vec{S} = \frac{c}{4\pi}\vec{E}\times\vec{B} \qquad \vec{E} = -\frac{1}{c}\vec{V}_{ph}\times\vec{B}$$

$$\vec{S}\cdot\vec{n}_{ph} = \frac{B_\perp^2}{4\pi}\vec{V}_{ph}\cdot\vec{n}_{ph} - \frac{\vec{B}\cdot\vec{n}_{ph}}{4\pi}\vec{V}_{ph\perp}\cdot\vec{B}$$

Emerging Flux **Waves and Turbulence**

Interchange reconnection as source of EM energy and mass flux to the wind

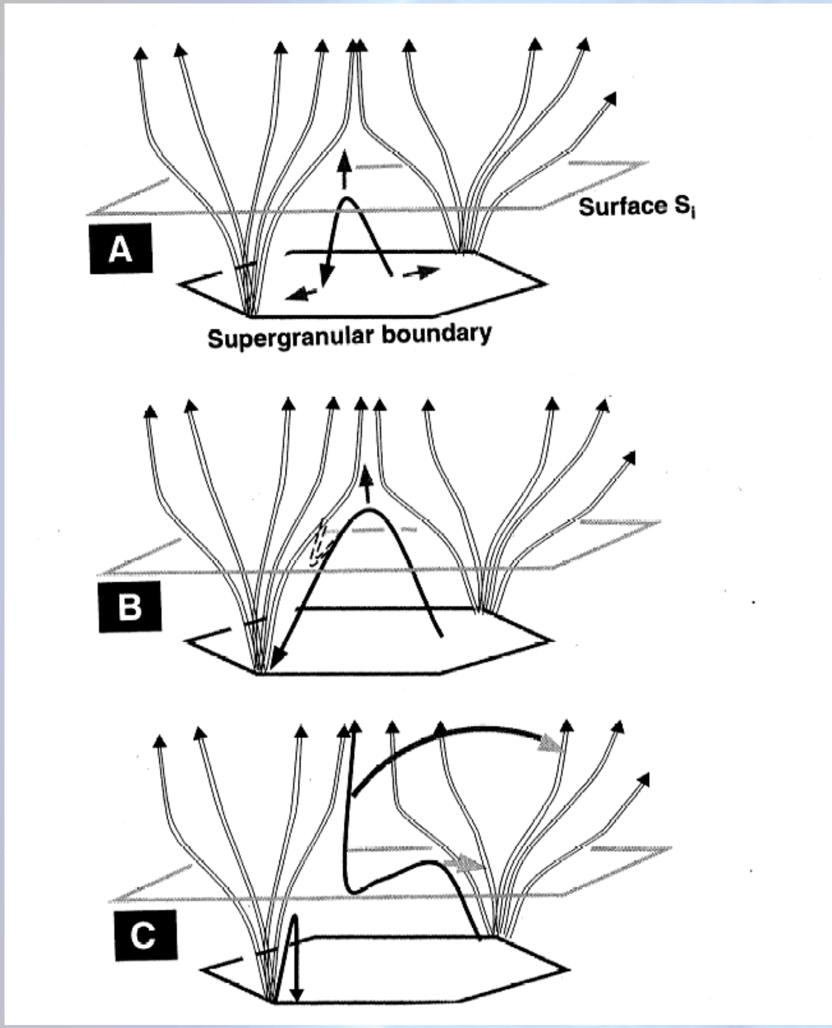

Fisk (2005)

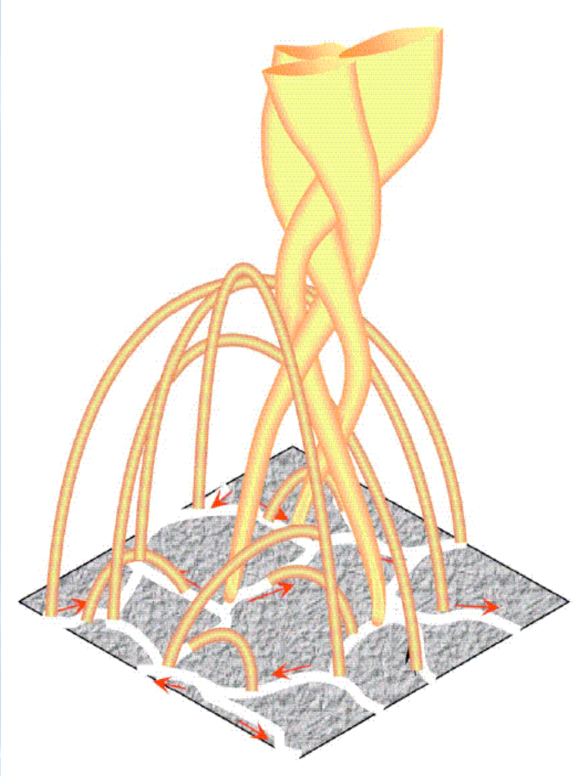

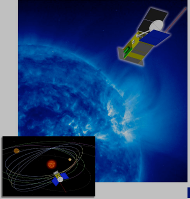

SW acceleration: Energy Balance Along a Flux Tube

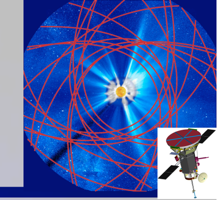

Source Mechanical flux (Coronal Heating+Pressure)
Conductive flux **Radiative** flux Solar Wind Flux:

$$F_{sw} = \dot{M}\left(\frac{V^2}{2} - \frac{V_g^2}{2} + \frac{5kT}{m_p}\right)$$

$$V_g = 618\ km/s$$

$$F_0 = F_{m,0} + \cancel{F_{q,0}} + \cancel{F_{rad,0}} - \dot{M}\frac{V_g^2}{2}$$

$$F_0 = F_{rad,\infty} + \dot{M}\frac{V_\infty^2}{2}$$

$$F_{m,0} = \dot{M}\left(\frac{V_\infty^2}{2} + \frac{V_g^2}{2}\right) + F_{rad,\infty}$$

$$\frac{V_\infty^2}{2} = \frac{1}{\dot{M}}\left(F_{m,0} - F_{rad,\infty}\right) - \frac{V_g^2}{2}$$

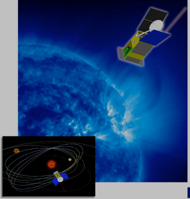

Coronal Heating and SW Acceleration 2

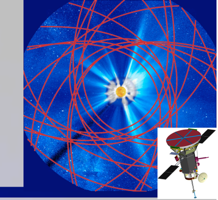

A very basic result (leads to "scaling laws" Fisk et al '99 Fisk '03):

$$\rho v r^2 f_{\rm tot} \frac{v^2}{2}\bigg|_{r=1\,\rm AU} = \left\{ r^2 \left[-\frac{B_r \langle \delta B_\perp \delta v_\perp \rangle}{4\pi} + \rho v \left(\frac{\gamma}{\gamma-1} R T_C - \frac{G M_\odot}{r} \right) \right] \right\}_{r=1\,R_\odot}. \tag{3}$$

Schwadron & McComas '03, '08

$$\frac{m u_f^2}{2} \approx m \bar{v}_{\rm A0}^2 - \left(C_0 \frac{\kappa_0 T_{\max}^{7/2}}{f_0 L} - C_1 k T_{\max} \right) - \frac{G M_\odot m}{R_\odot} \ .$$

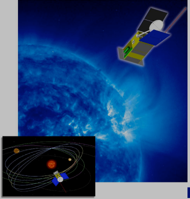

Schwadron & McComas '08

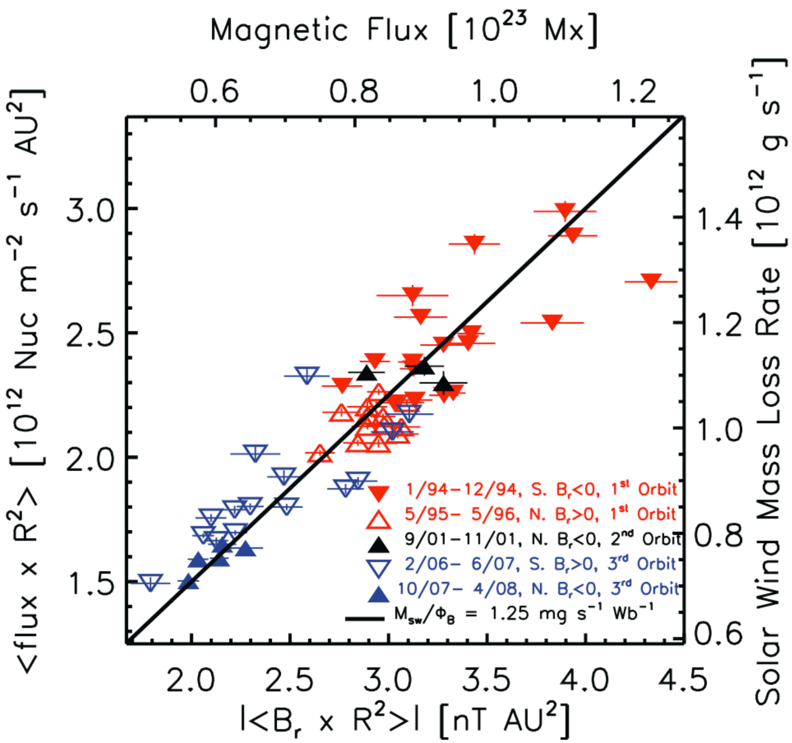

FIG. 1.—Solar wind mass flux vs. the magnitude of the magnetic flux density, $|\langle \bar{B} \rangle|$, in the *Ulysses* polar regions for latitudes above $\pm 40°$ and for solar wind speeds >710 km s^{-1}. We have included the solar wind He^{++} flux in these estimates. The left-hand vertical scale shows the radially normalized average mass flux, while the right-hand scale multiplies by the area of a sphere at 1 AU to form the total mass-loss rate. Similarly, the lower horizontal scale applies to the magnetic flux density, while the upper scale applies to the total magnetic flux. The black line from the model of Schwadron & McComas (2003) model with a mass-loss rate per magnetic flux of 1.25 mg s^{-1} Wb^{-1} matches the observations remarkably well.

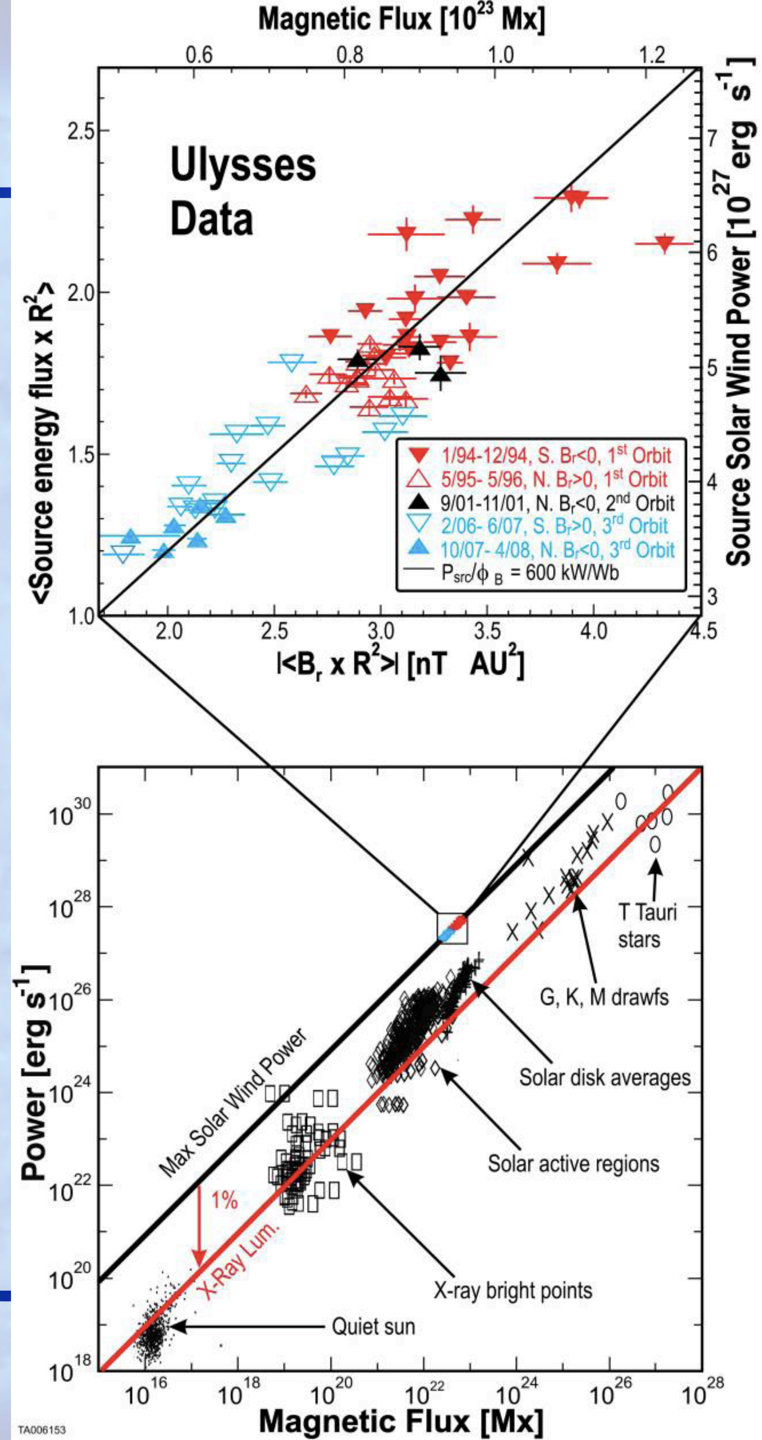

Evolution of waves in turbulence from coronal holes into the fast wind

Can a turbulence theory work in coronal holes to heat and drive the solar wind? Incompressible: invoke REFLECTION of ALFVEN WAVES (Velli et al. 1989, Matthaeus et al 2000, Verdini et al. '05, Cranmer et al. '05)
Compressible: +
Nonlinear Steepening

- Generation of waves by foot point motion
- Reflection of the waves due to variation of Va
- Turbulent cascade, plasma heating and wind acceleration in perpendicular planes

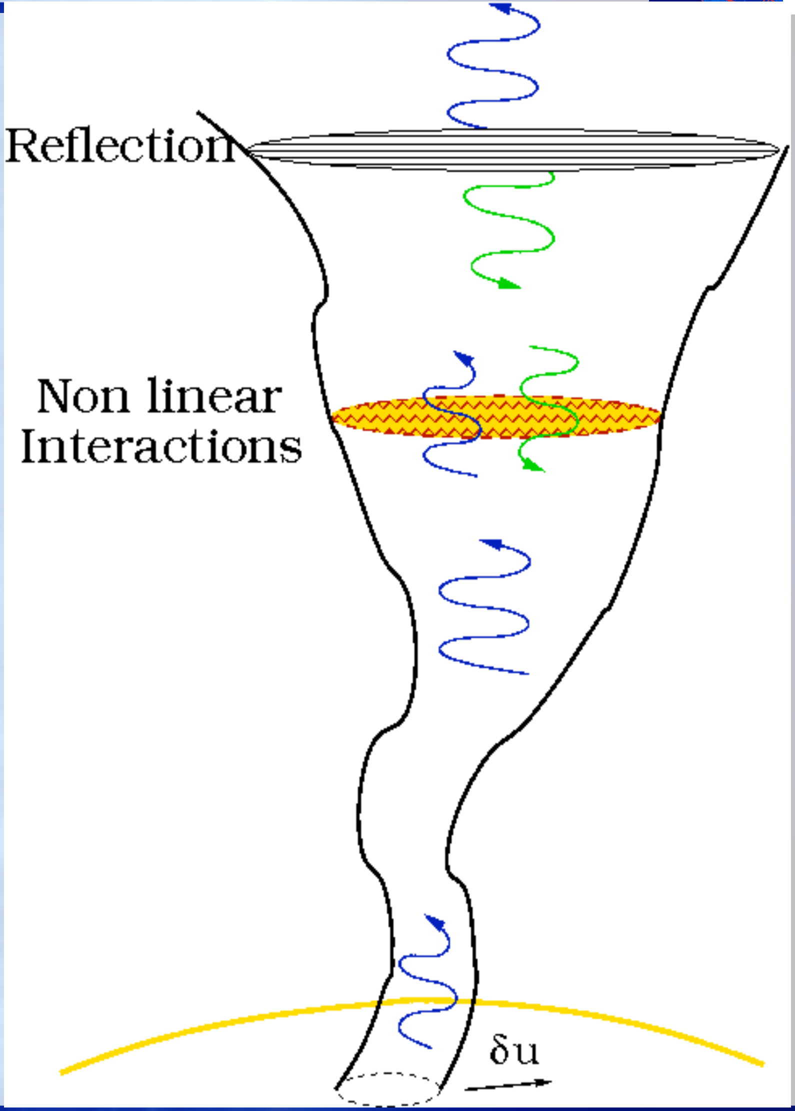

Evolution of waves in turbulence from coronal holes into the fast wind

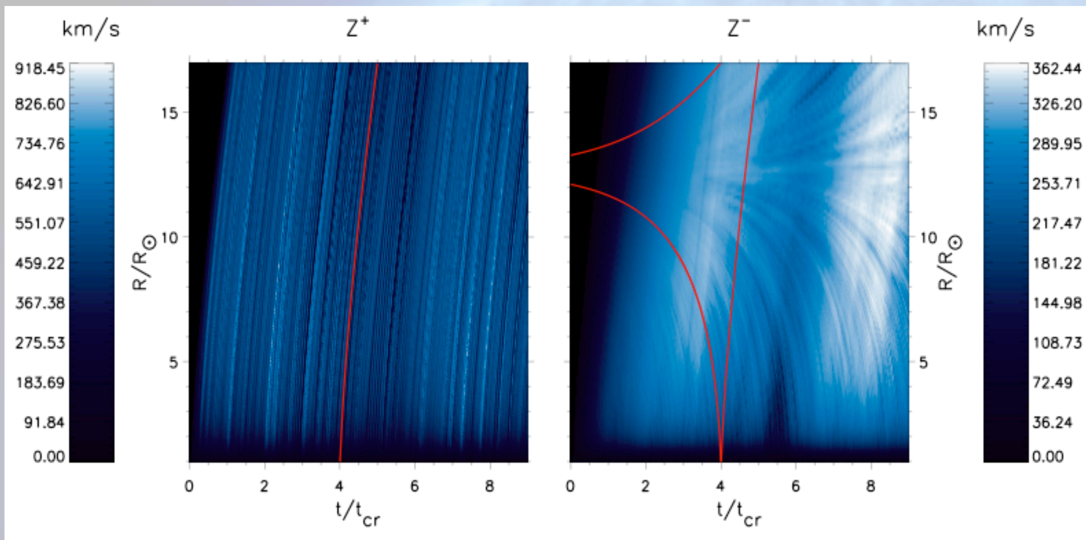

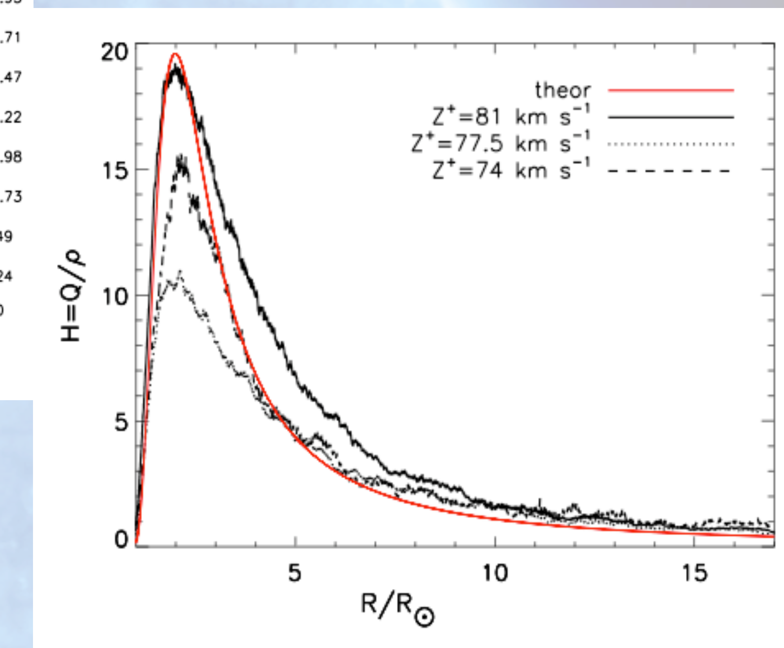

Generation of waves by foot point motion. Reflection of the waves due to variation of Va.Turbulent cascade, plasma heating and wind acceleration in perpendicular planes (Verdini & Velli, 2007, 2009).

Evolution of waves in turbulence from coronal holes into the fast wind

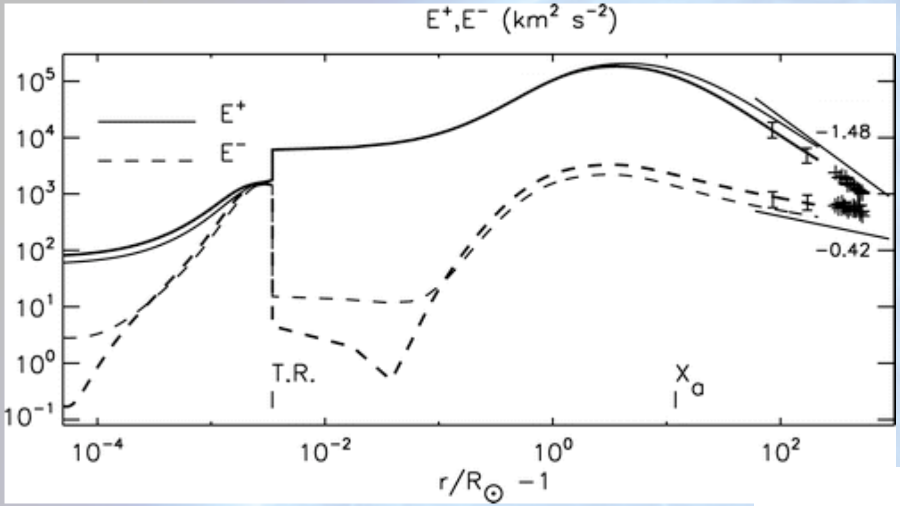

Energies/mass as a function of heliocentric distance

Rms u and b as a function of heliocentric distance

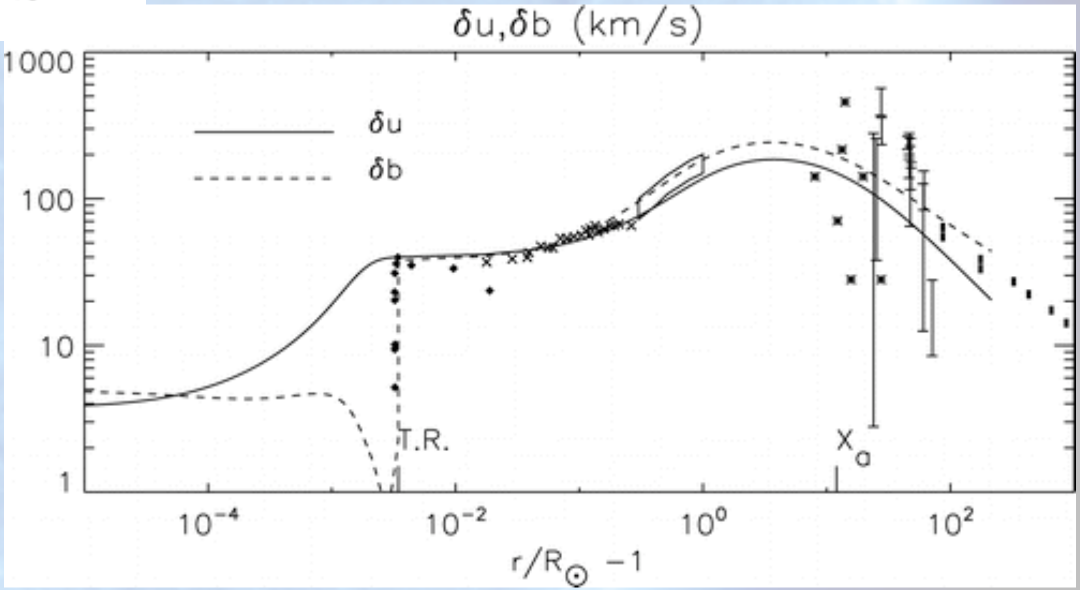

Suzuki et al '05 - '07

Comparison of fast and slow winds obtained with circularly polarized Alfvén wave forcing.

Alfvén waves drive and reflect off density gradients, parametric decay et.c. generate compressive motions which shock and heat. So Alfvén waves push and shock waves push and heat.

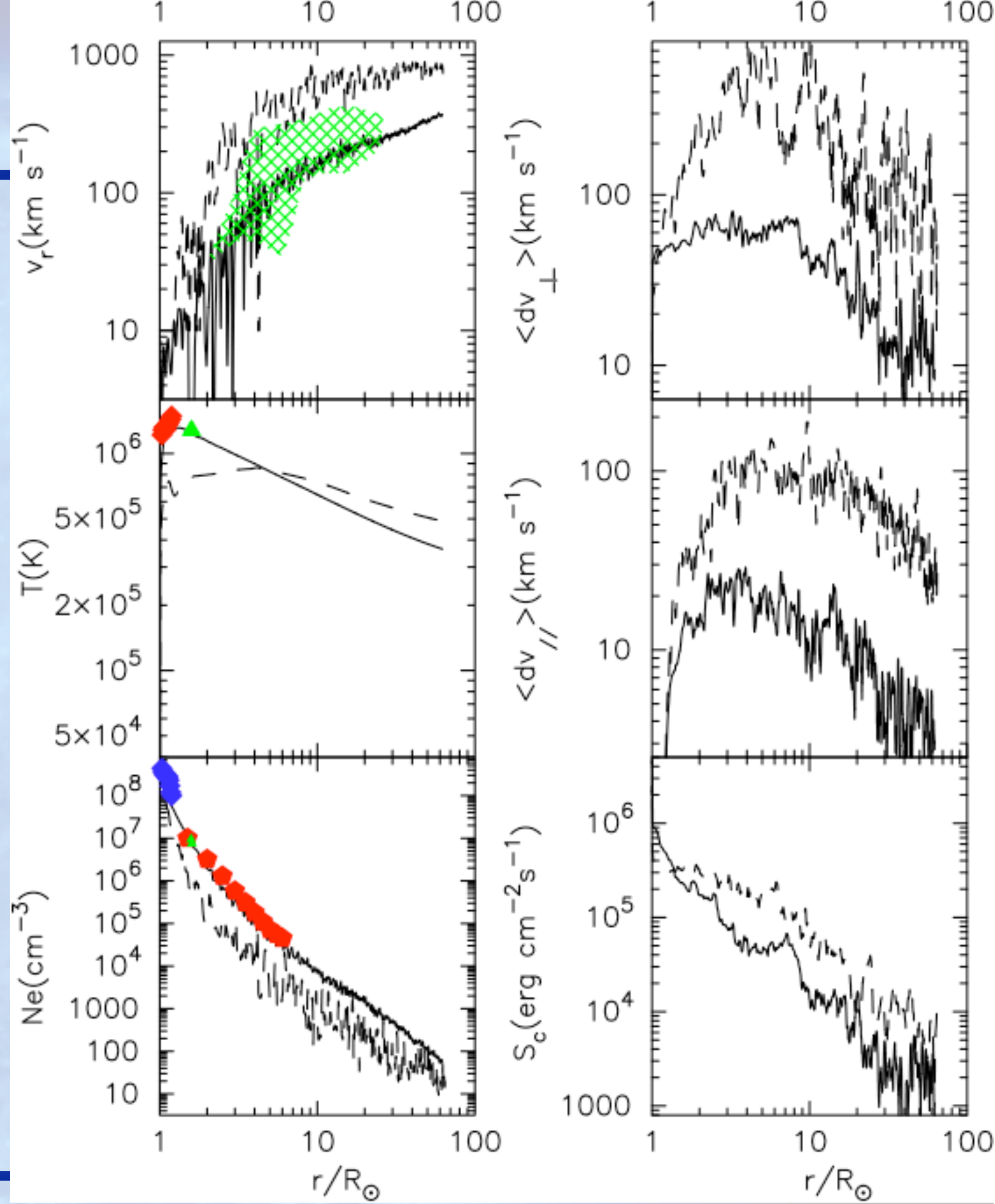

Solar wind is basically traced back radially to the source surface (2.something solar radii) and then back

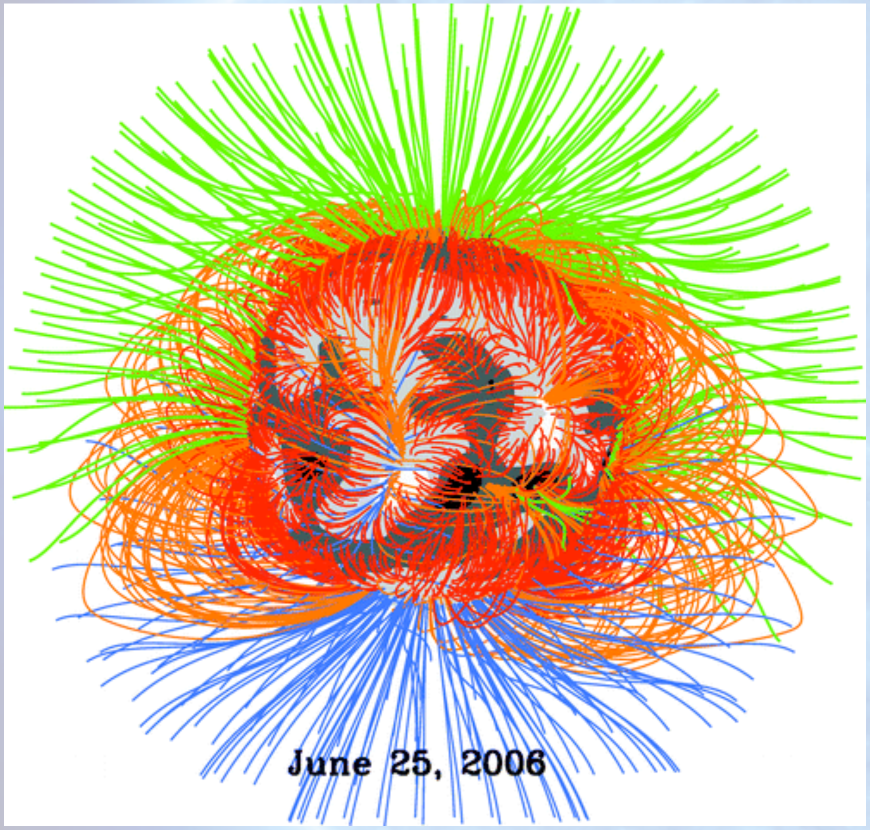

using a Potential Field Source Surface approximation.

One of the open questions is the precise location of open field regions.

Slow and fast wind: connectivity

High-speed wind: strong connections to the largest coronal holes

Low-speed wind: still no agreement on the full range of coronal sources:

- hole/streamer boundary (streamer "edge")
- streamer plasma sheet ("cusp/stalk")
- small coronal holes
- active regions

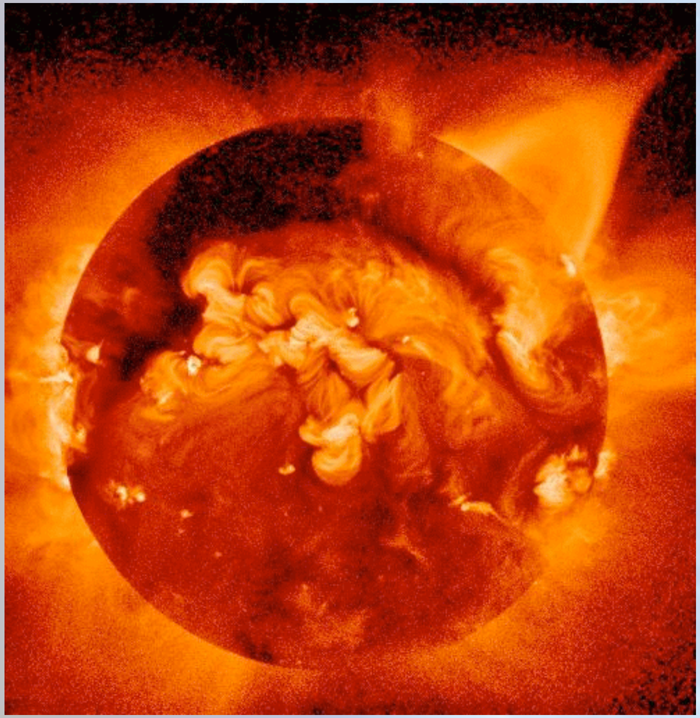

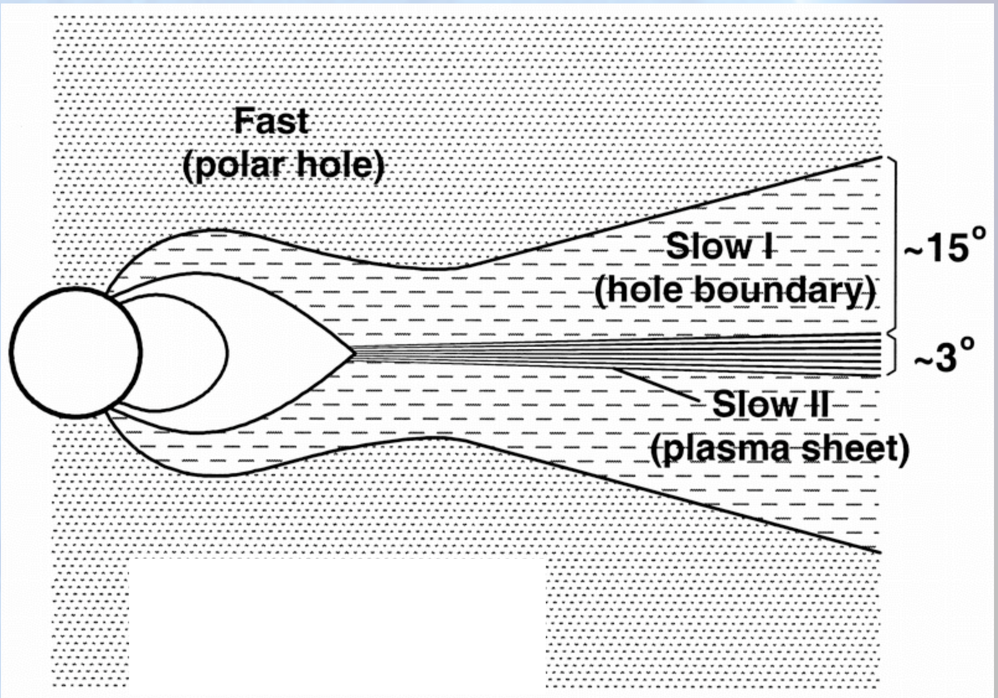

The Slow Solar Wind

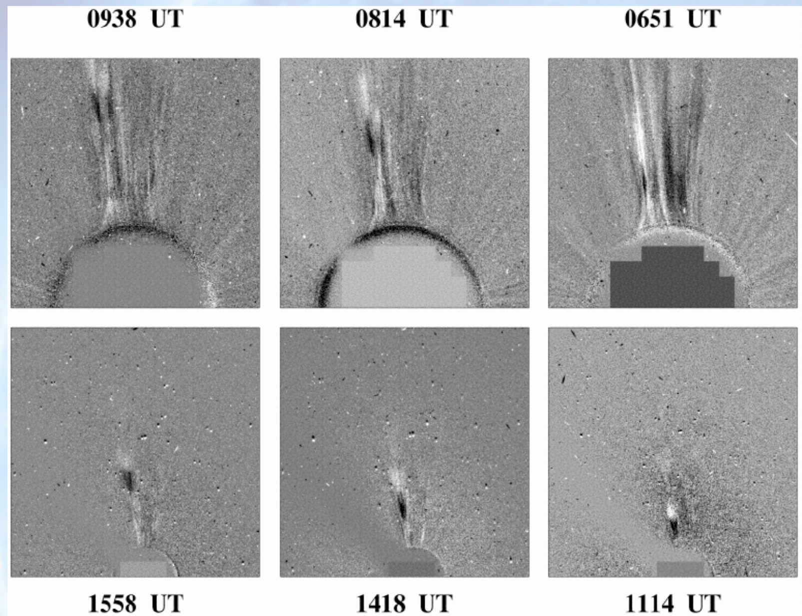

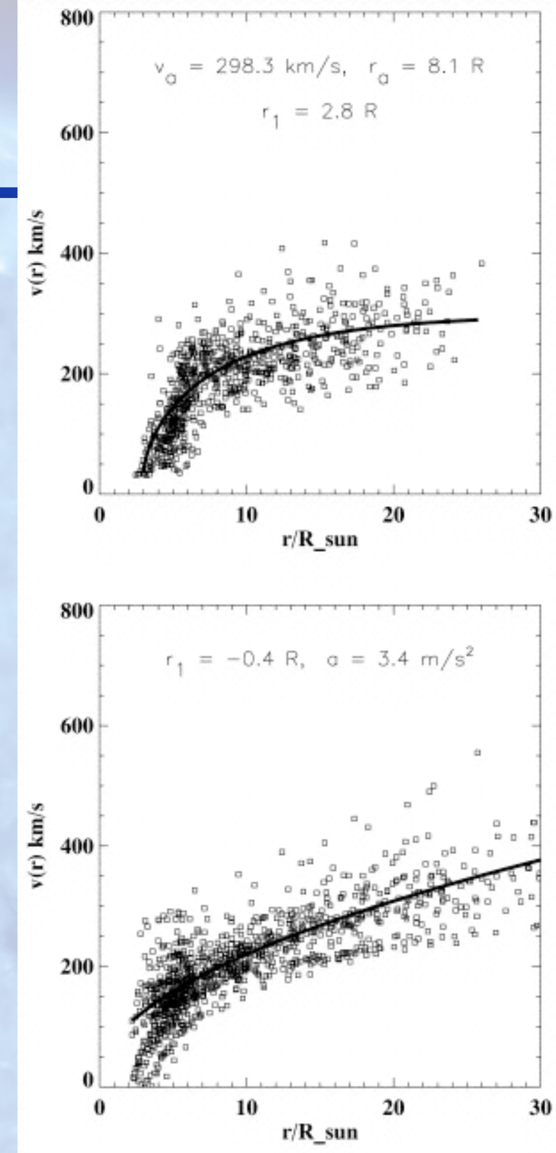

Time difference images showing flow of material in streamers

Sheeley, et al., 1997

Corresponding velocity profiles

Global magnetic field connectivity

Cranmer & van Ballegooijen ('07,'05) models of the global properties of incompressible non-WKB Alfvenic turbulence along an open flux tube.

Lower boundary condition: observed horizontal motions of G-band bright points.Along the flux tube, wave/turbulence properties should be computed consistently.

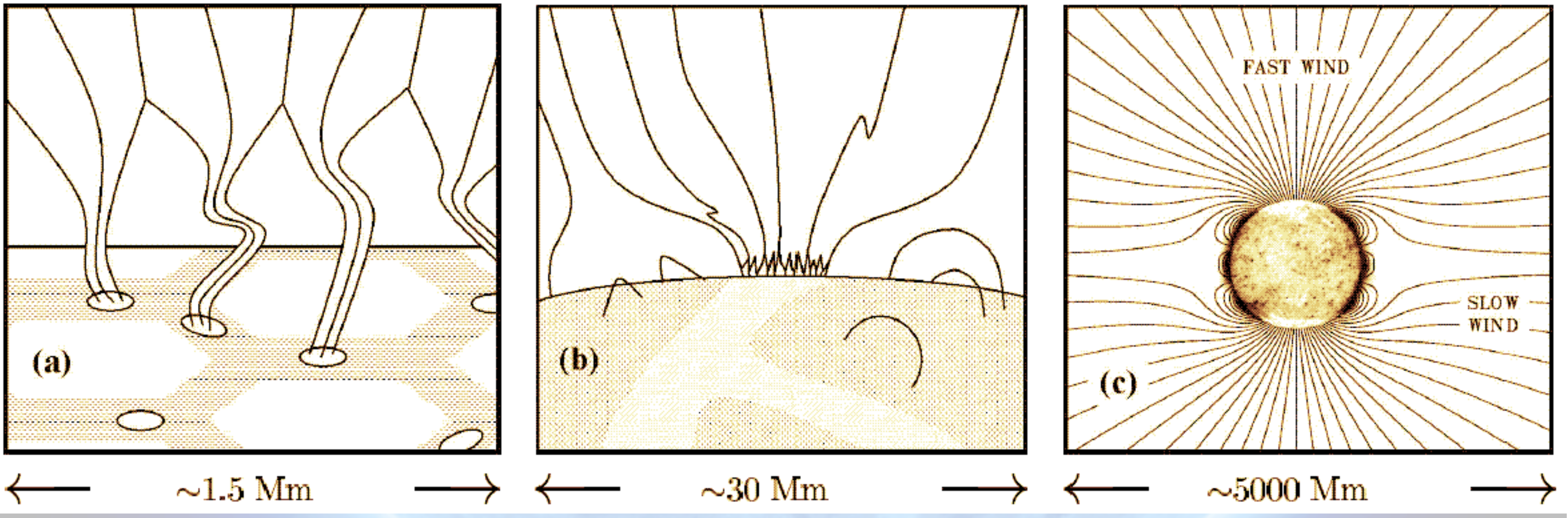

Slow Wind Origin from Expanding Flux Tubes

For a polar coronal hole flux-tube:

Basal acoustic flux: 10^8 erg/cm^2/s (equiv. "piston" v = 0.3 km/s)

Basal Alfvenic perpendicular amplitude: 0.4 km/s

Basal turbulent scale: 120 km (G-band bright point size)

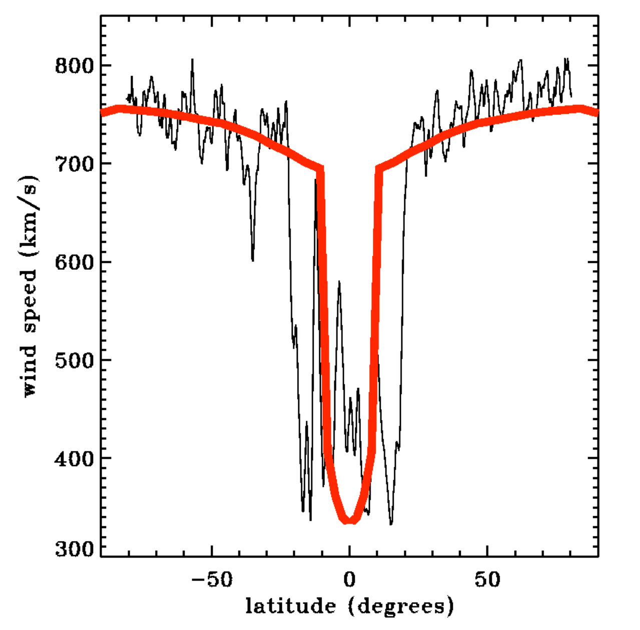

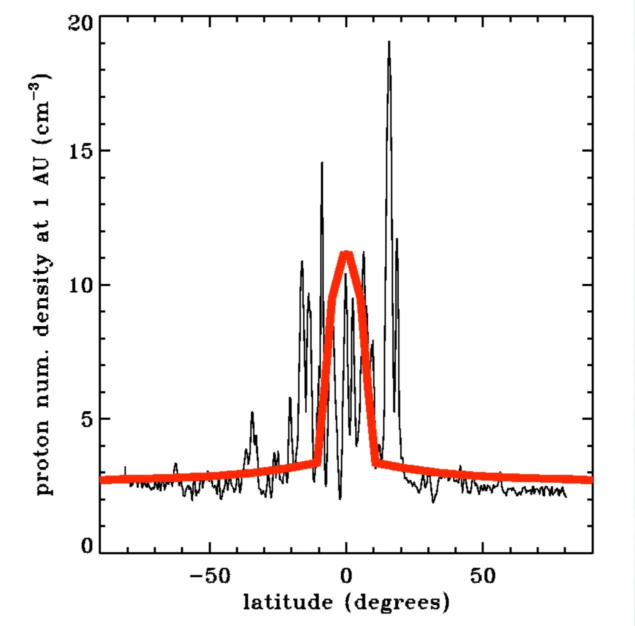

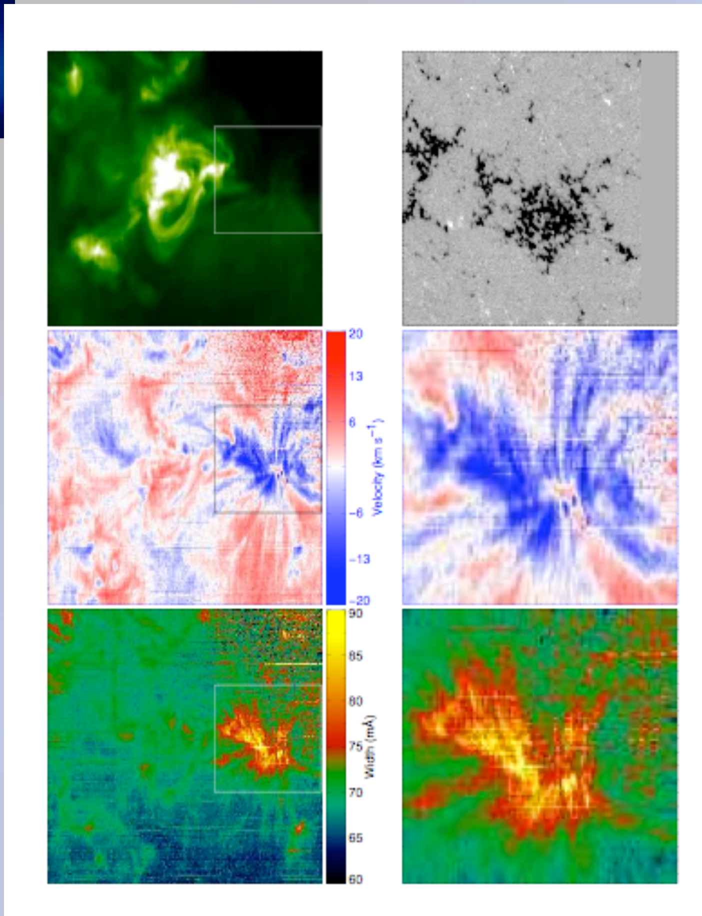

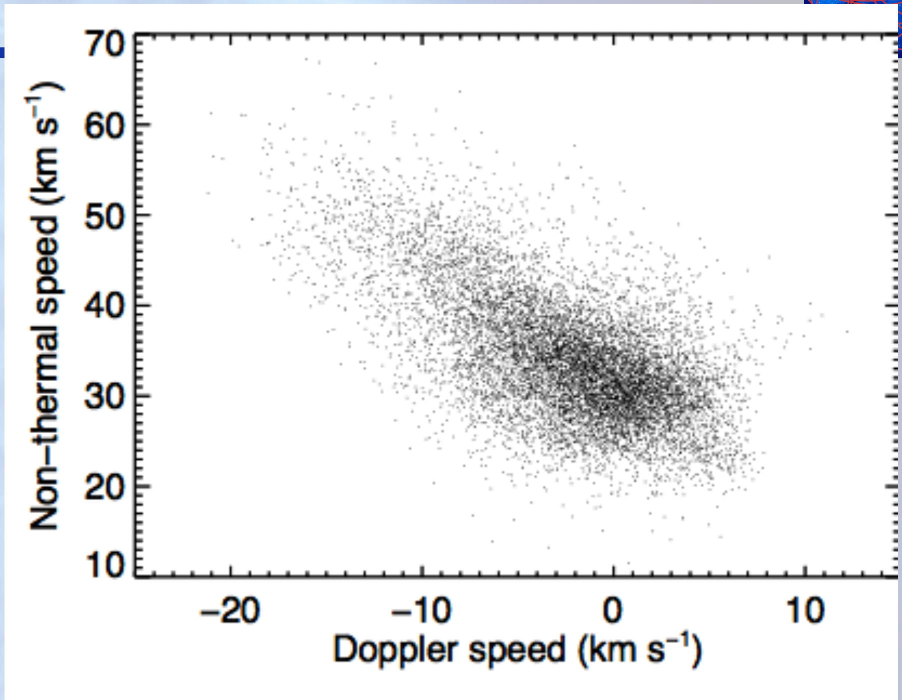

The locations of the flows in the active regions with respect to the longitudinal photospheric magnetic fields suggest that these regions might be tracers of long loops and/or open magnetic fields that extend into the heliosphere, and thus the flows could possibly contribute significantly to the solar wind. (Doschek et al 08)

Origins of the slow wind

Endeve et al 2004

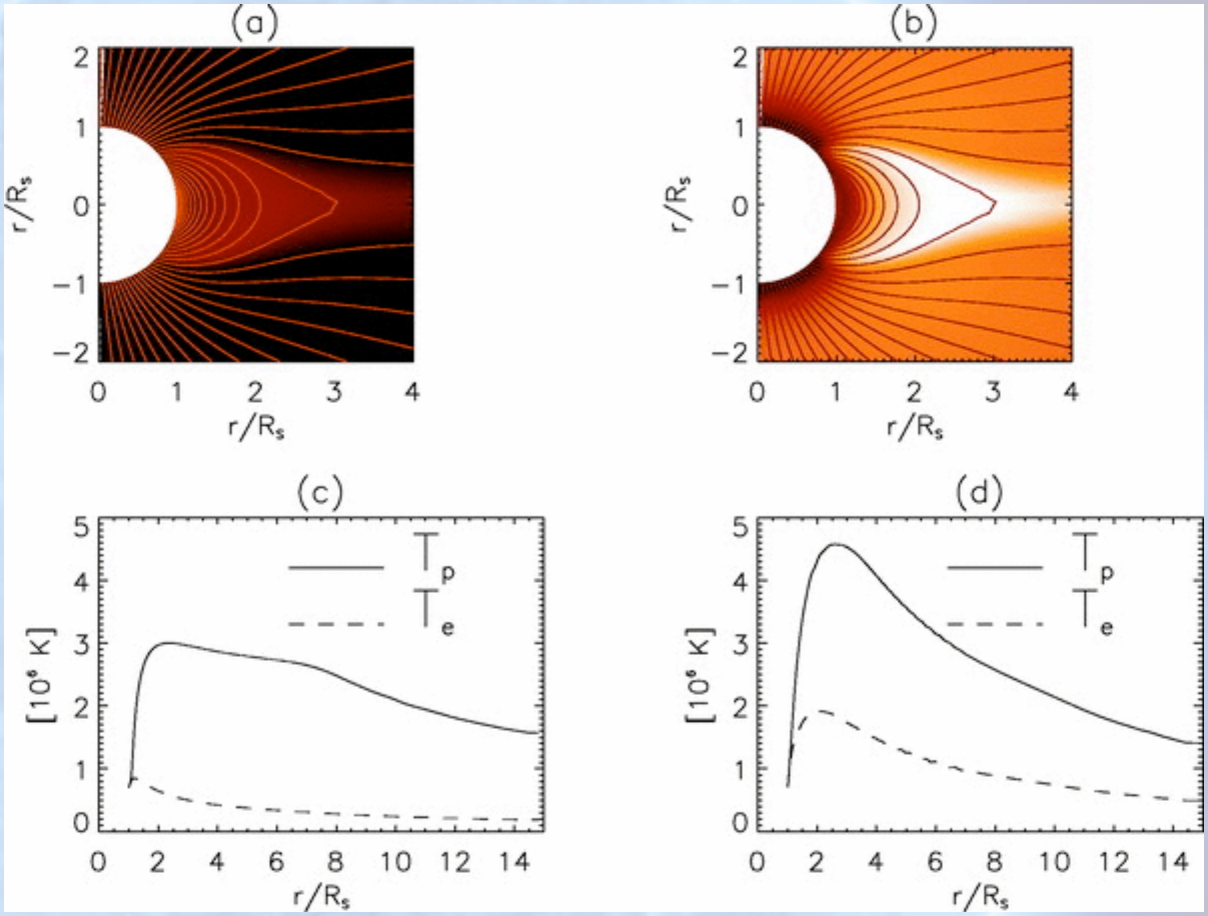

Snapshot of the coronal temperature structure for the base model, in which only protons are heated. (a, b) Color plots of the electron and proton temperature, respectively. Solid lines are for overlying magnetic field structure. (c, d) Electron (dashed line) and proton (solid line) temperatures vs. heliocentric distance along (c) the polar axis and (d) the equator.

Origins of the slow wind

Depending on heating partition, no stationary state is found

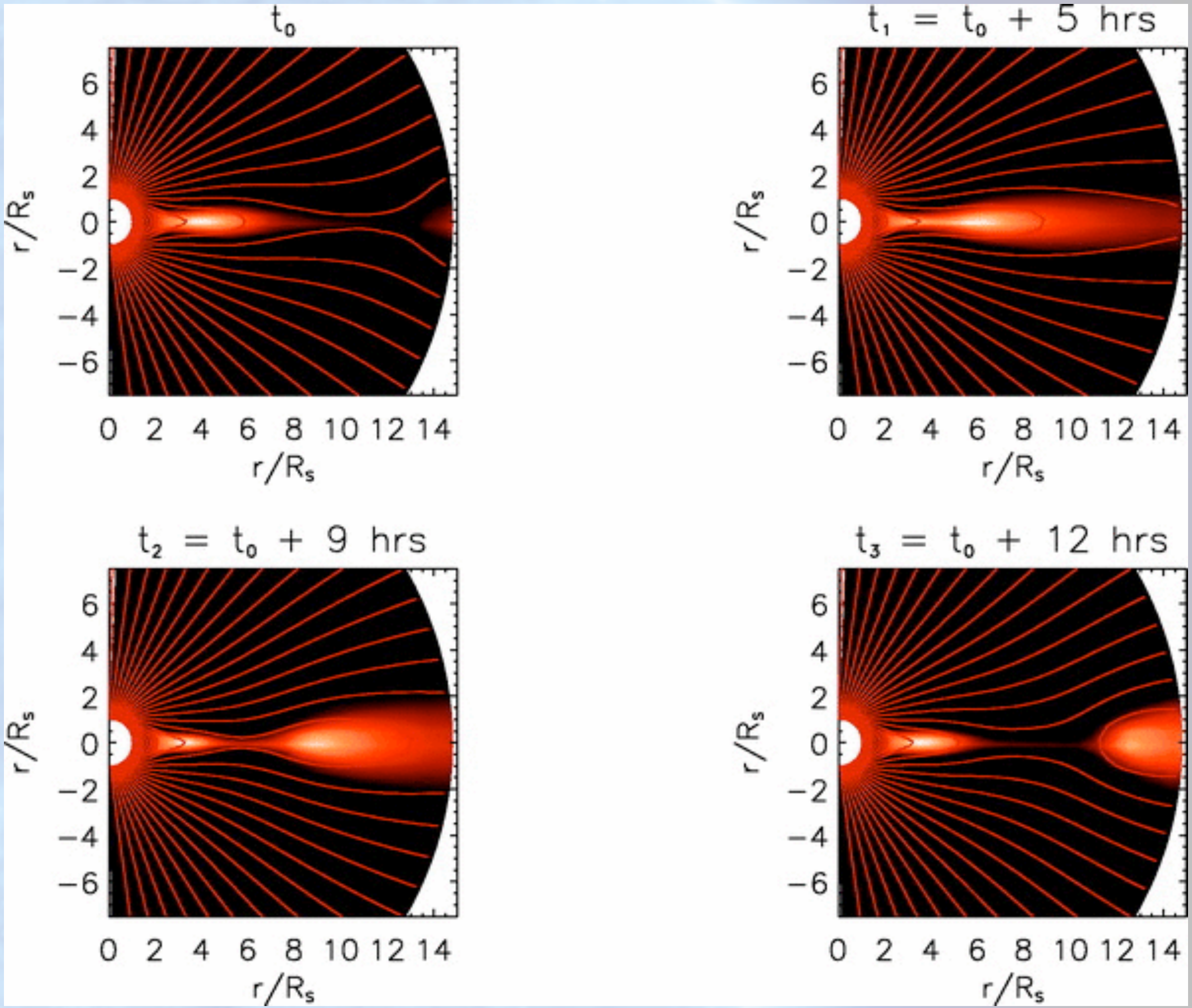

The solar wind texture at L1

Figure 1. A sketch of the flux tube texture of the solar-wind plasma. Each flux tube contains a different plasma and the flux tubes move independently. A depiction (left) looking at the sides of the tubes indicates that the tubes are tangled about the direction of the Parker spiral. An end view (right) depicts the cross sections of the network of tubes. The scale sizes of the flux tubes correspond to the scale sizes of granules on the solar surface. The median diameter of a flux tube at 1 AU is 5.5×10^5 km.

The Solar Wind at HELIOS: Pressure-balanced S

"It is now fairly well established that high-speed streams are partly composed of mesoscale flow tubes which are related to coronal fine structures and seem to reflect in their angular scales of 2o-4o in Carrington longitude the sized of single or several supergranular cells of the chromospheric network on the Sun."* Thieme et al. 1989,, Schwenn and Marsch 1991

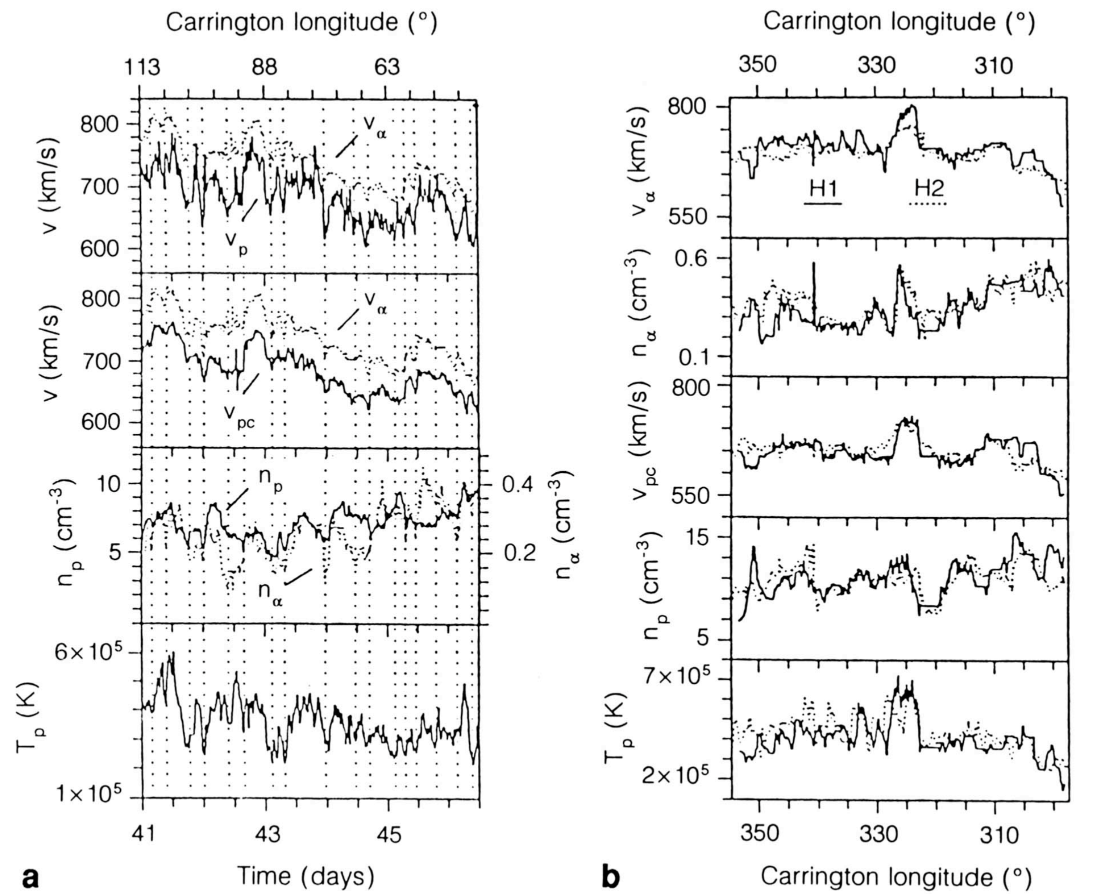

Fig. 10.2. (**a**) Velocities, densities, and temperatures of protons and α-particles from day 41 until day 46.5 in 1975, as measured by *Helios 1* between 0.6 and 0.66 AU. This fast stream shows significant related variations of the plasma parameters. The boundaries of the mesoscale flow tubes are marked by *dotted vertical lines*. (**b**) The plasma line-up around day 69.5 in 1976. The data of *Helios 2* (*dotted curves*) have been projected on the orbit of *Helios 1* by taking radial gradients into account. Radially invariant spatial structures are clearly revealed [10.173, 174]

The Fast Solar Wind at ULYSSES: switchbacks

- The fast solar wind carries magnetic field lines with a polarity which corresponds to the dominant polarity in the photosphere

- Observations show a number of cases where the magnetic field is reversed.

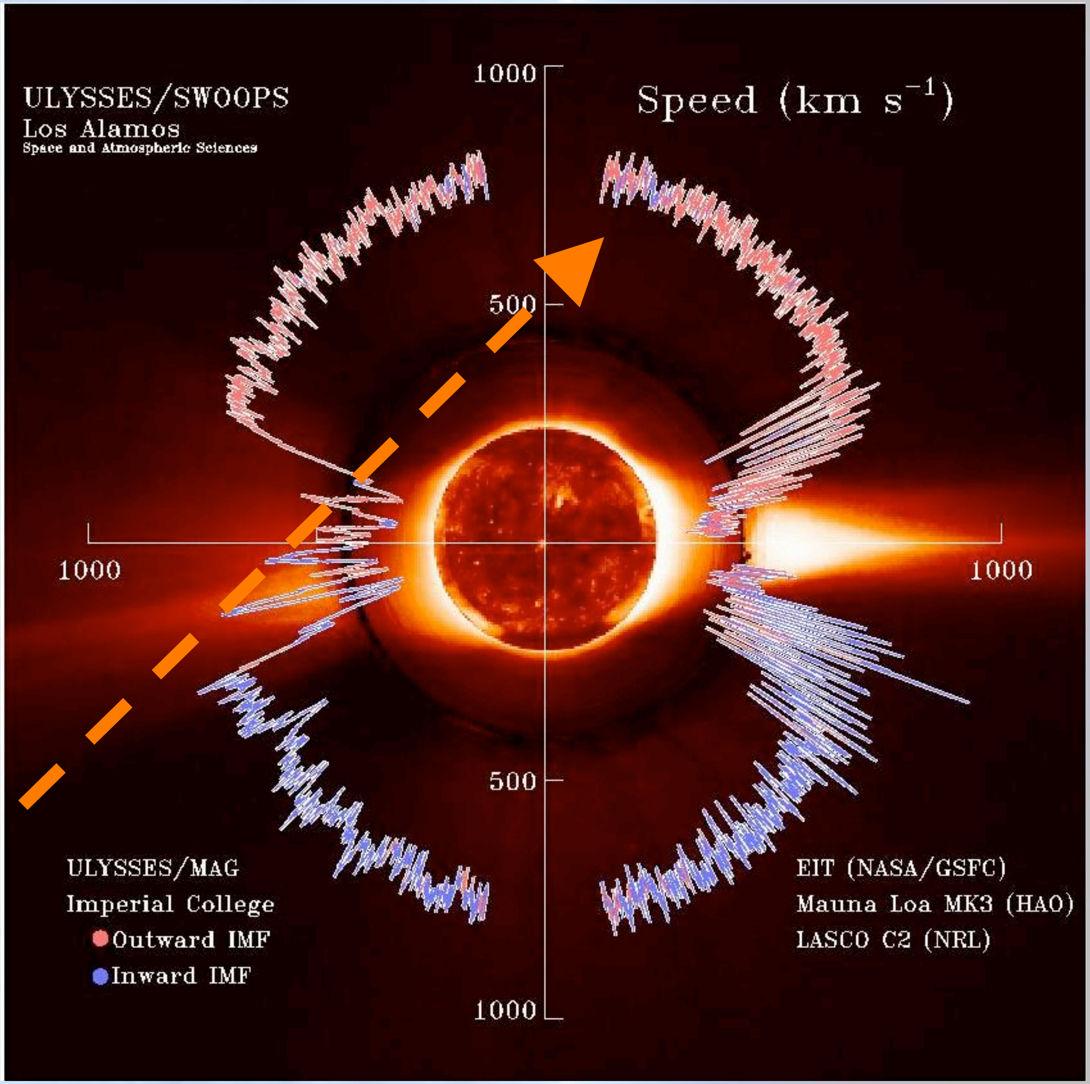

Formation of switchbacks: a way to see plumes?

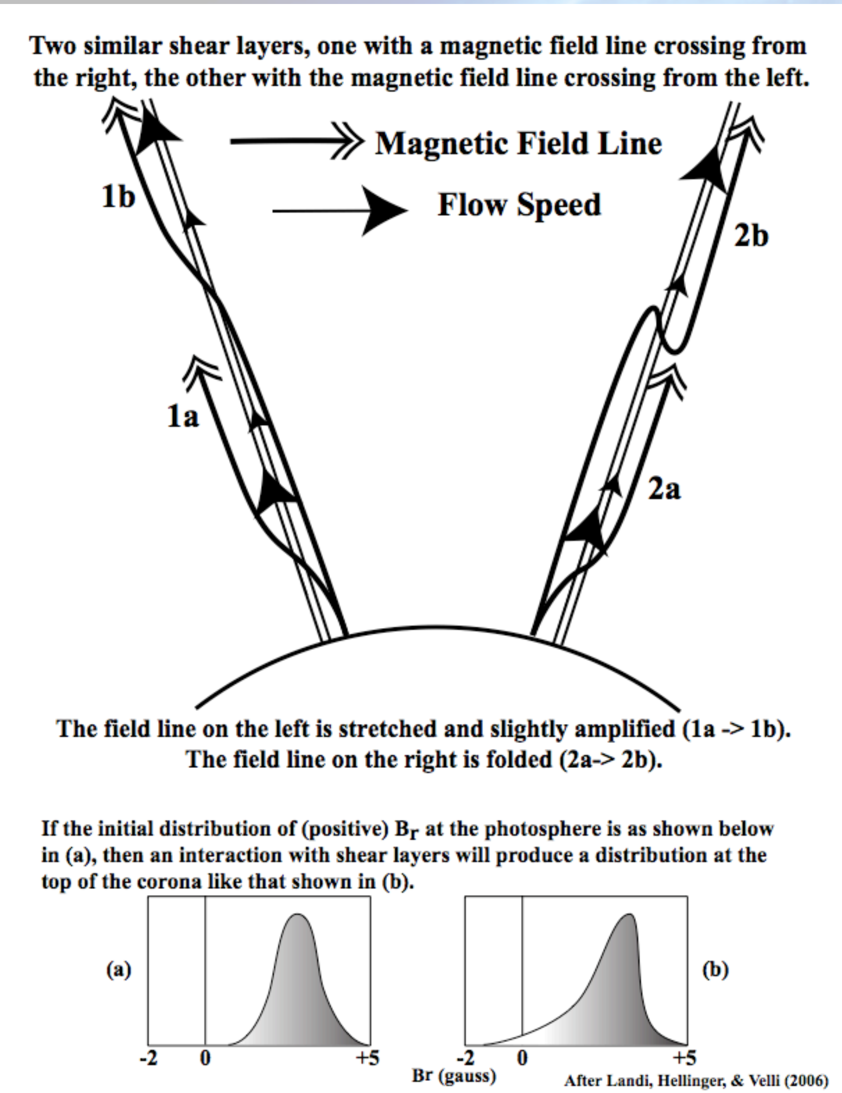

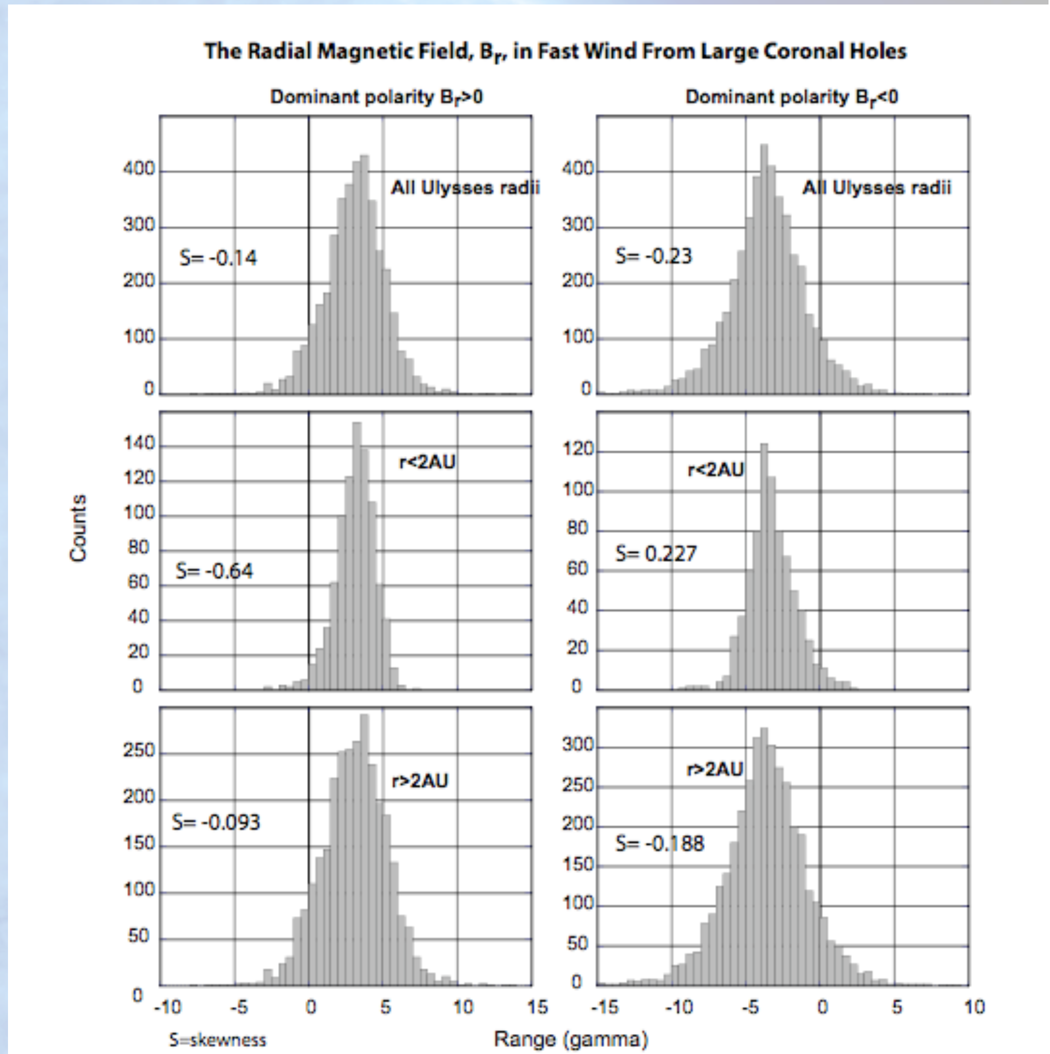

Landi et al. 07, Suess et al. ‘09

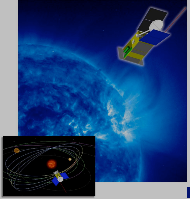

By way of Conclusion

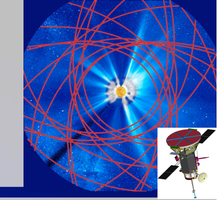

We are beginning to have predictive models of solar wind conditions, but the precise mechanisms of transfer of momentum and energy in all but the simplest open field configurations remain largely unknown.

On the one hand, we need to understand the inner boundary condition (photosphere/chromosphere/transition region in its 3 dimensional time-dependent nature) Hinode, SDO, Solar Orbiter

On the other, we need to understand the energy conversion channels inside the corona. Solar Probe.

Finally, we need to observe the magnetic field and flows at all latitudes on the sun.

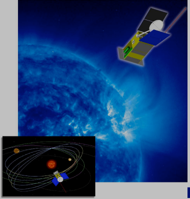

FUTURE

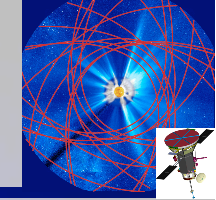

- Understand fully compressible MHD, and inclusion of emerging flux.
- Improved understanding of the reconnection process: kinetic, particle acceleration, convergence of kinetic and fluid solar wind models

New Missions with synergistic REMOTE SENSING and IN SITU OBSERVATIONS INSIDE ALFVEN POINT will solve the heating and acceleration problem

Solar Orbiter & Solar Probe

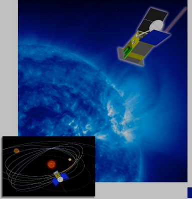

To investigate solar atmospheric coupling: remote sensing. Solar Dynamics Observatory and Solar Orbiter

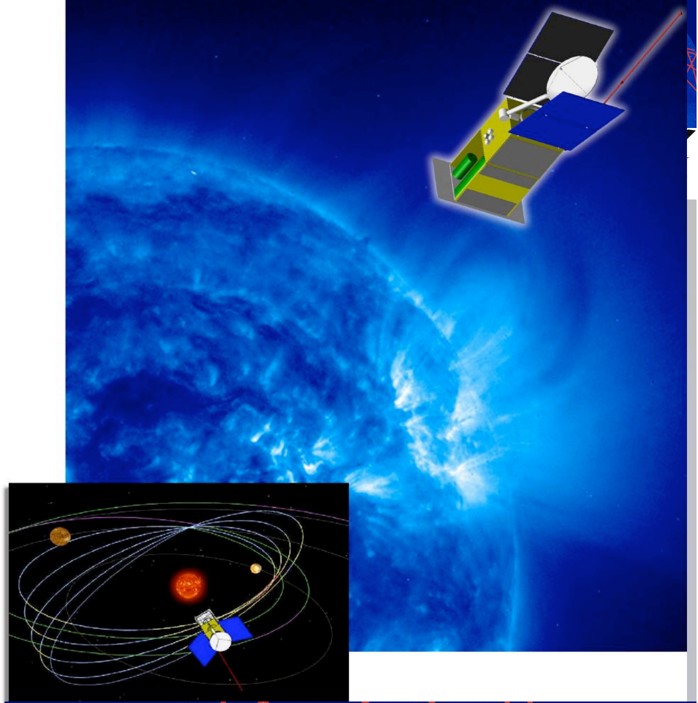

To investigate the coronal heating and the acceleration of the solar wind: Solar Probe (+)